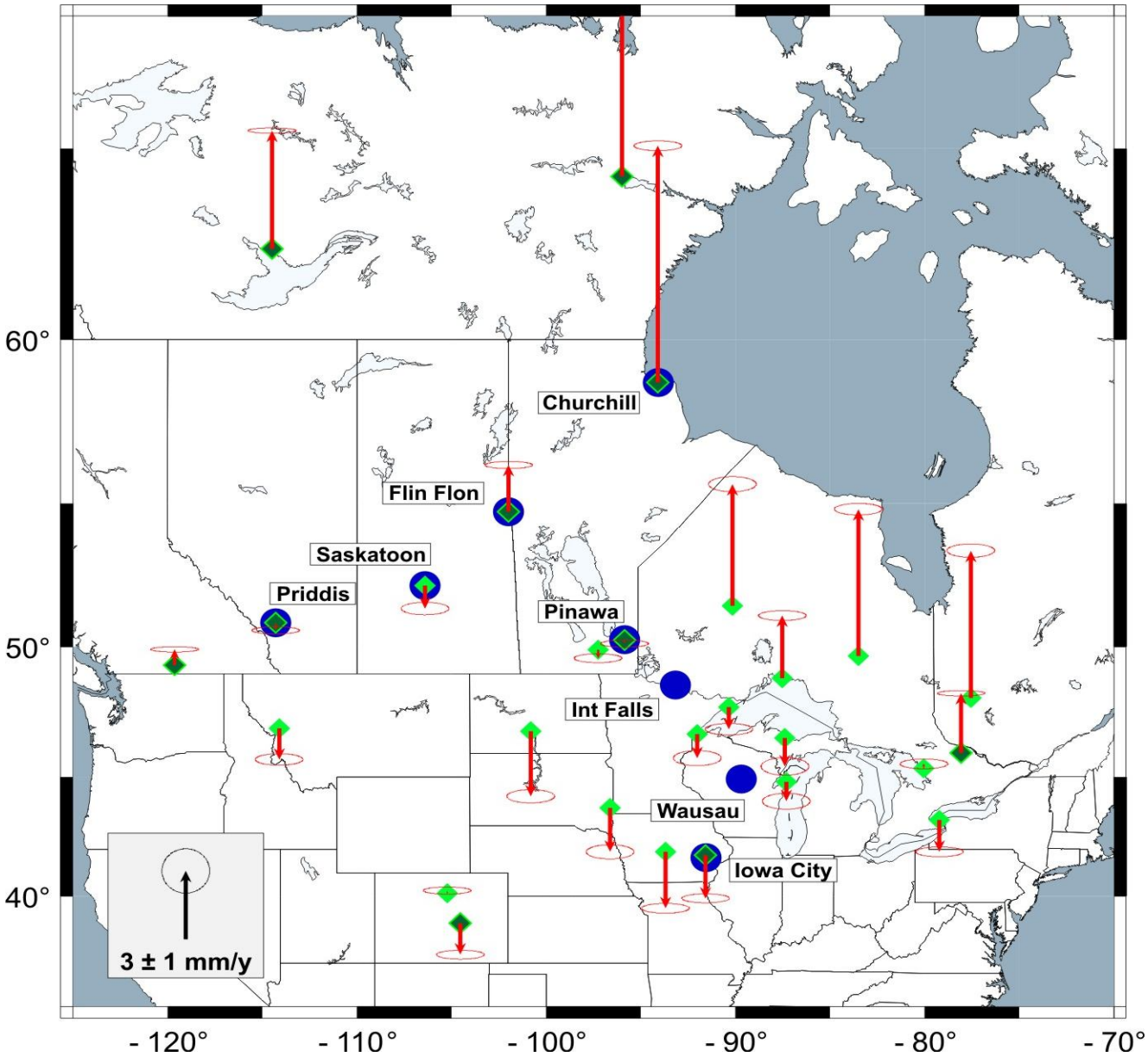

Figure 1a. North-American mid-continent absolute gravity and continuous GPS stations. Blue dots show absolute gravity stations. Dark and light green diamonds show fiducial and unconstrained GPS stations, respectively. Red arrows show vertical velocities (up positive) and their 95% confidence interval, aligned to ITRF2005.

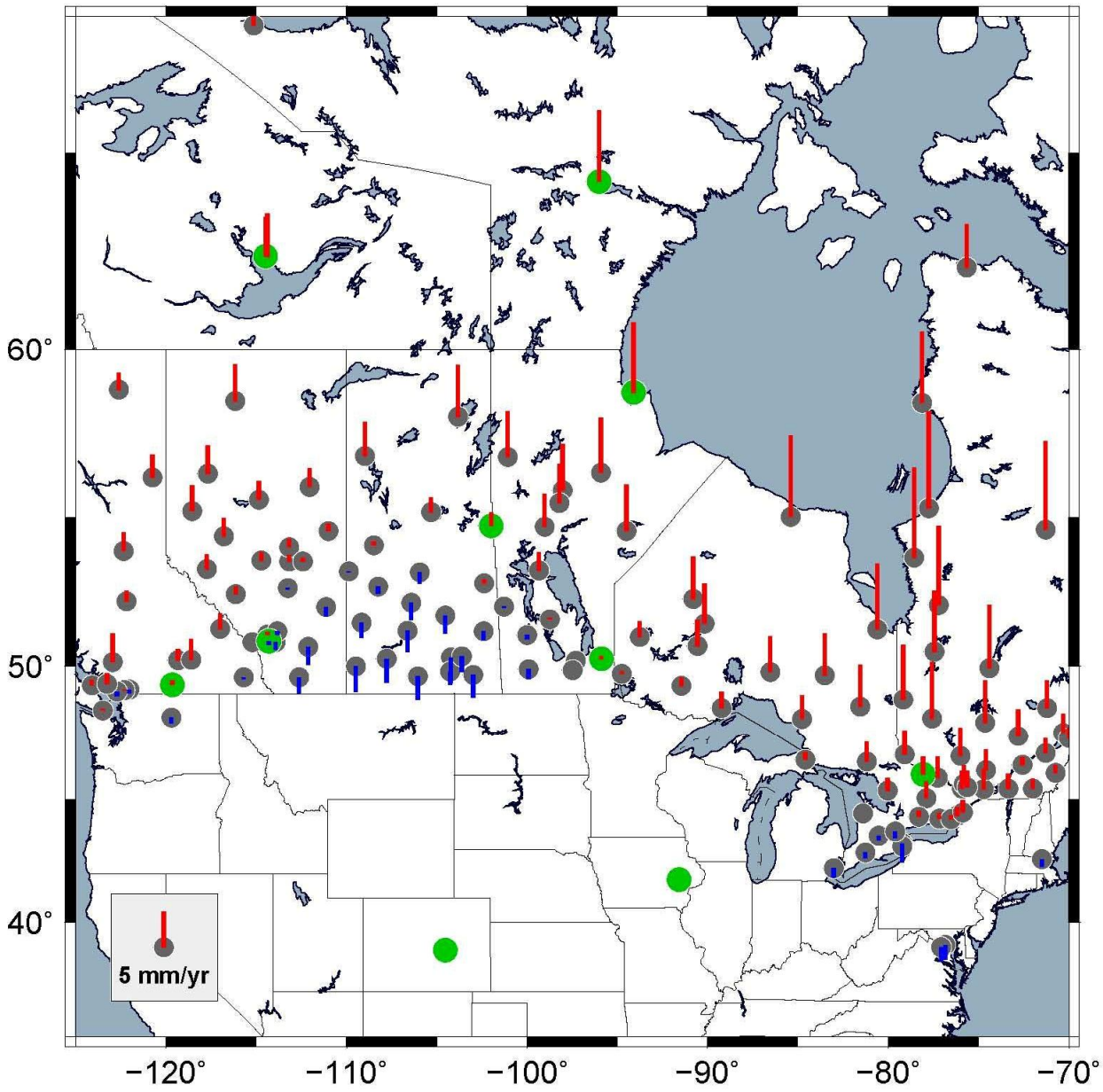

Figure 1b. North-American mid-continent Canadian Base Network (CBN) stations. Red and blue arrows show vertical velocities (red-up and blue-down) aligned to the ITRF2005. Green dots indicate reference, continuous GPS stations. Results from this "campaign-style" CBN network have been combined with the results from the continuous GPS network shown in Fig. 1a.

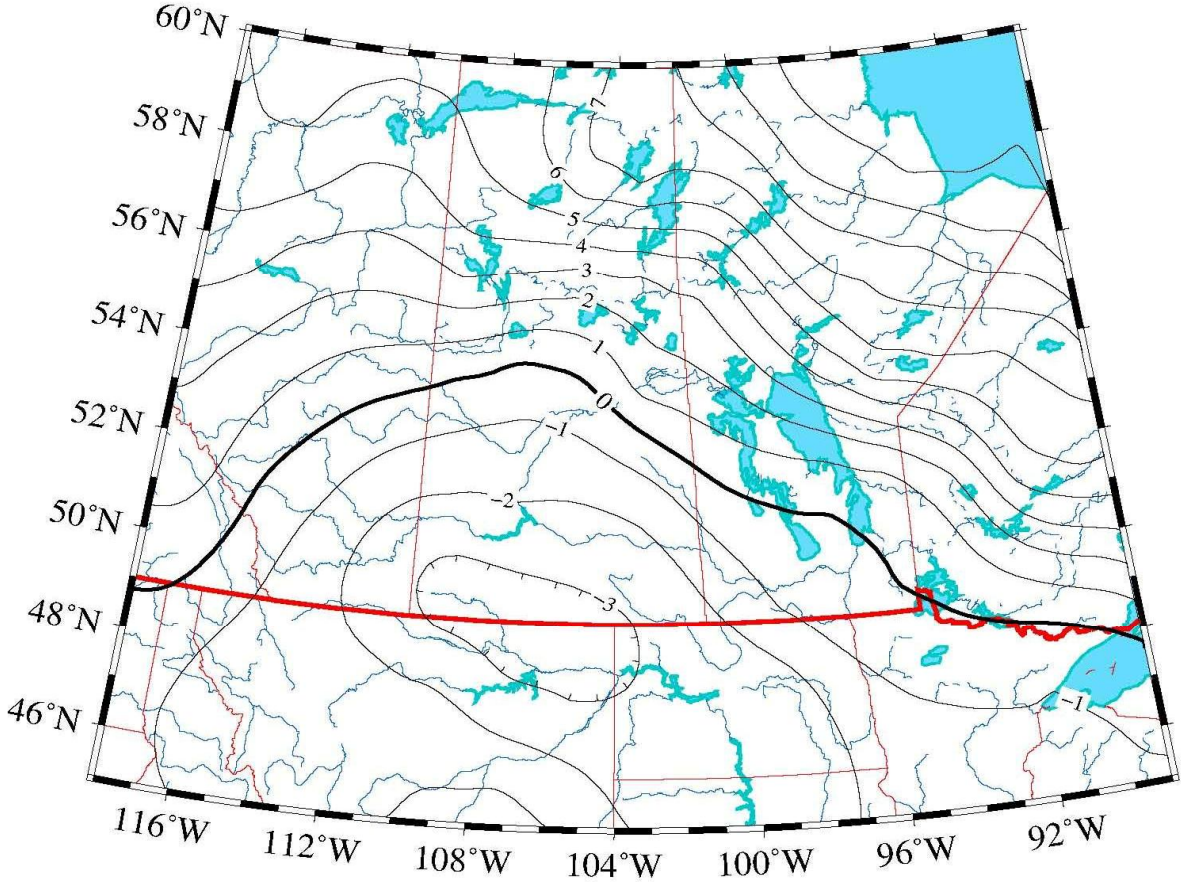

Figure 2. Vertical crustal velocity map for the Nelson River drainage basin derived from GPS observations. The units are mm/yr and up is positive.

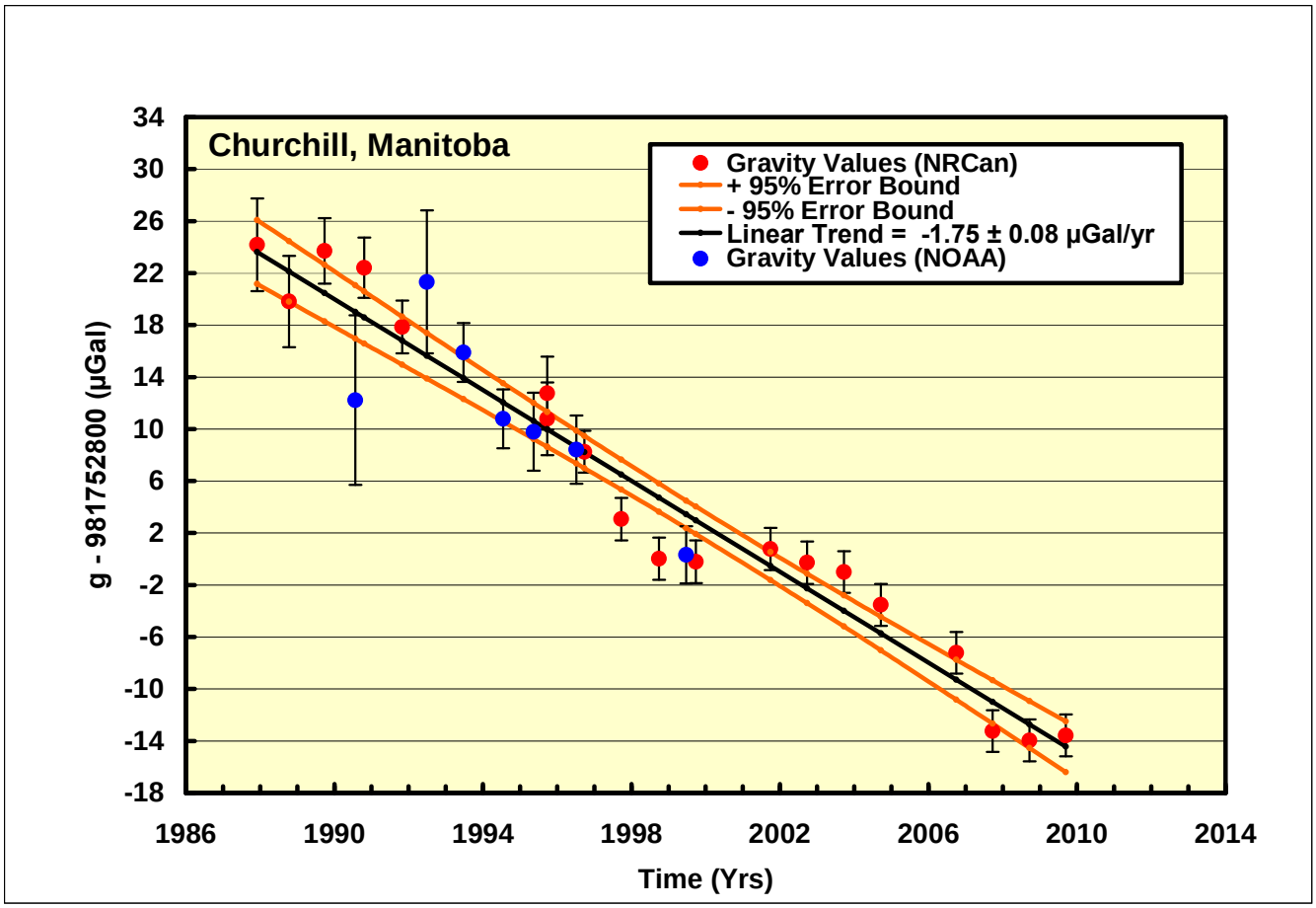

Figure 3a. Observed gravity at Churchill, Manitoba. Error bars denote standard errors.

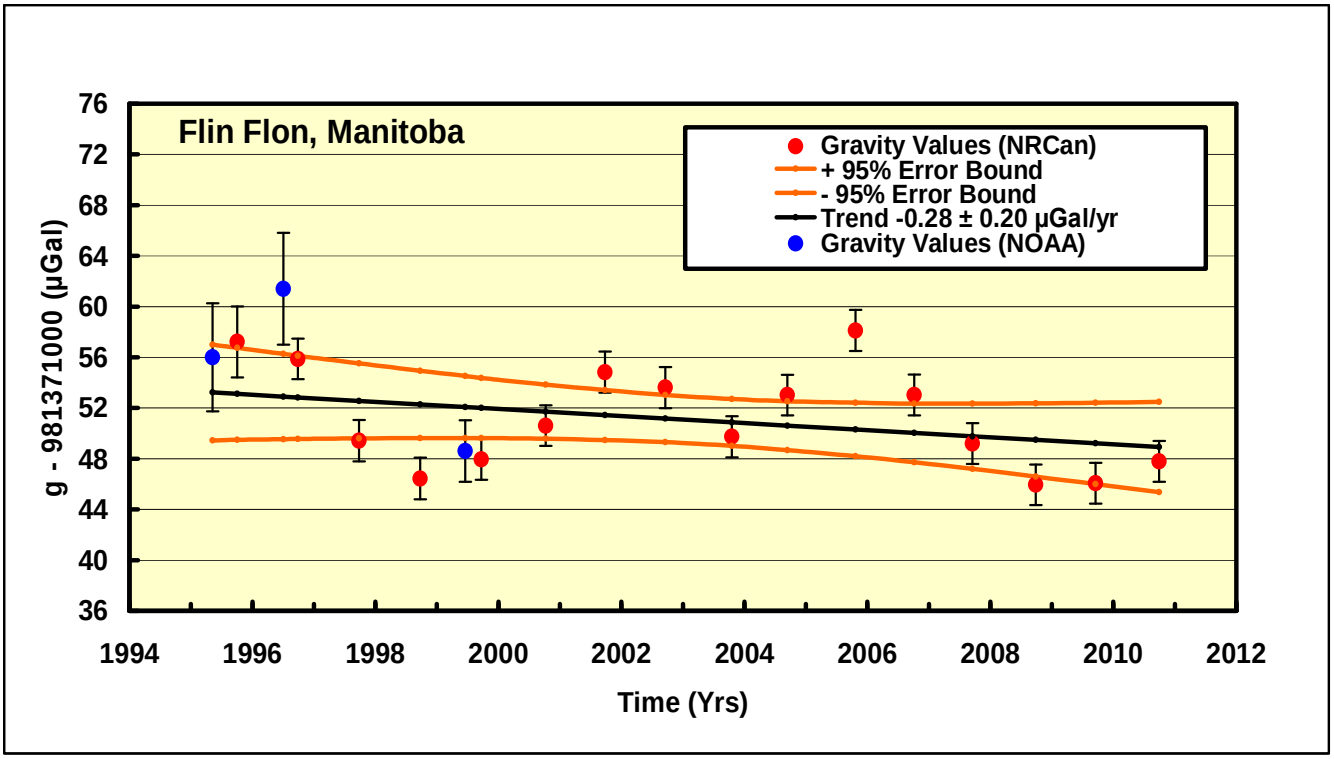

Figure 3b. Observed gravity at Flin Flon, Manitoba. Error bars denote standard errors.

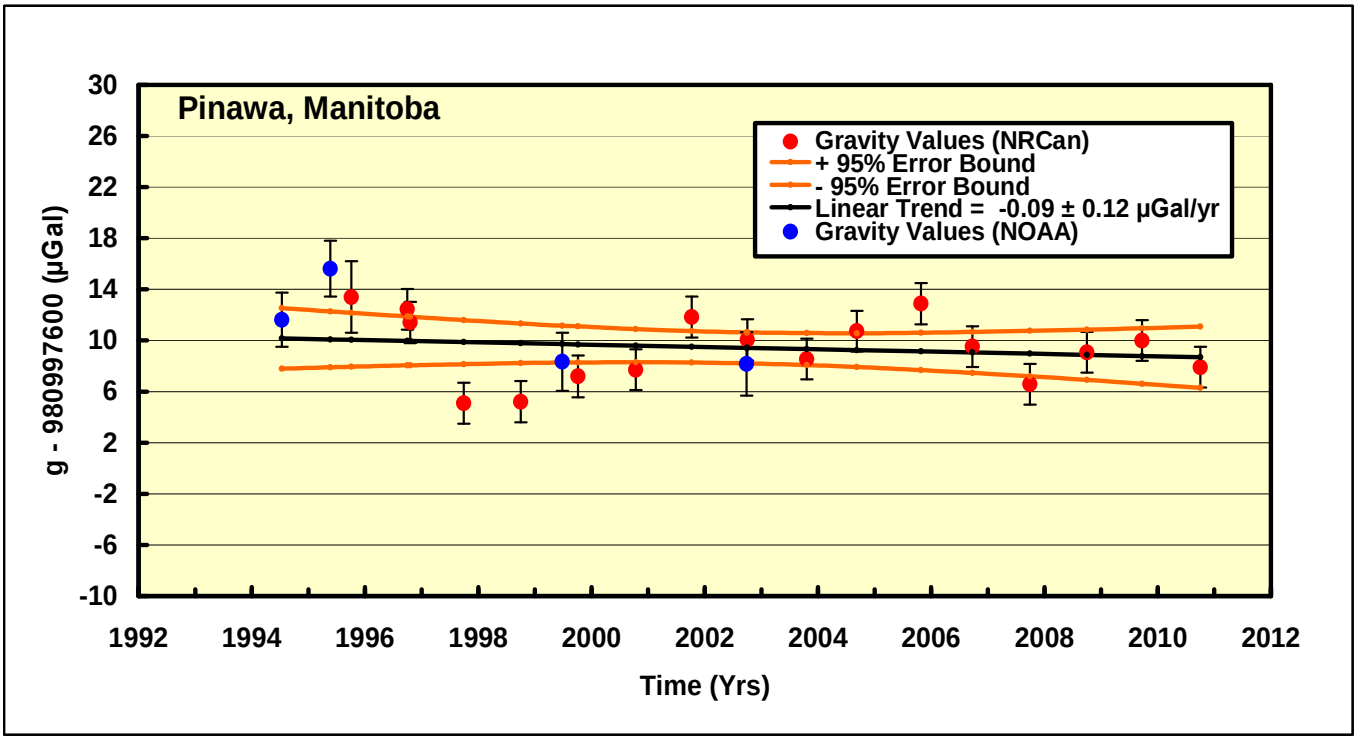

Figure 3c. Observed gravity at Pinawa, Manitoba. Error bars denote standard errors.

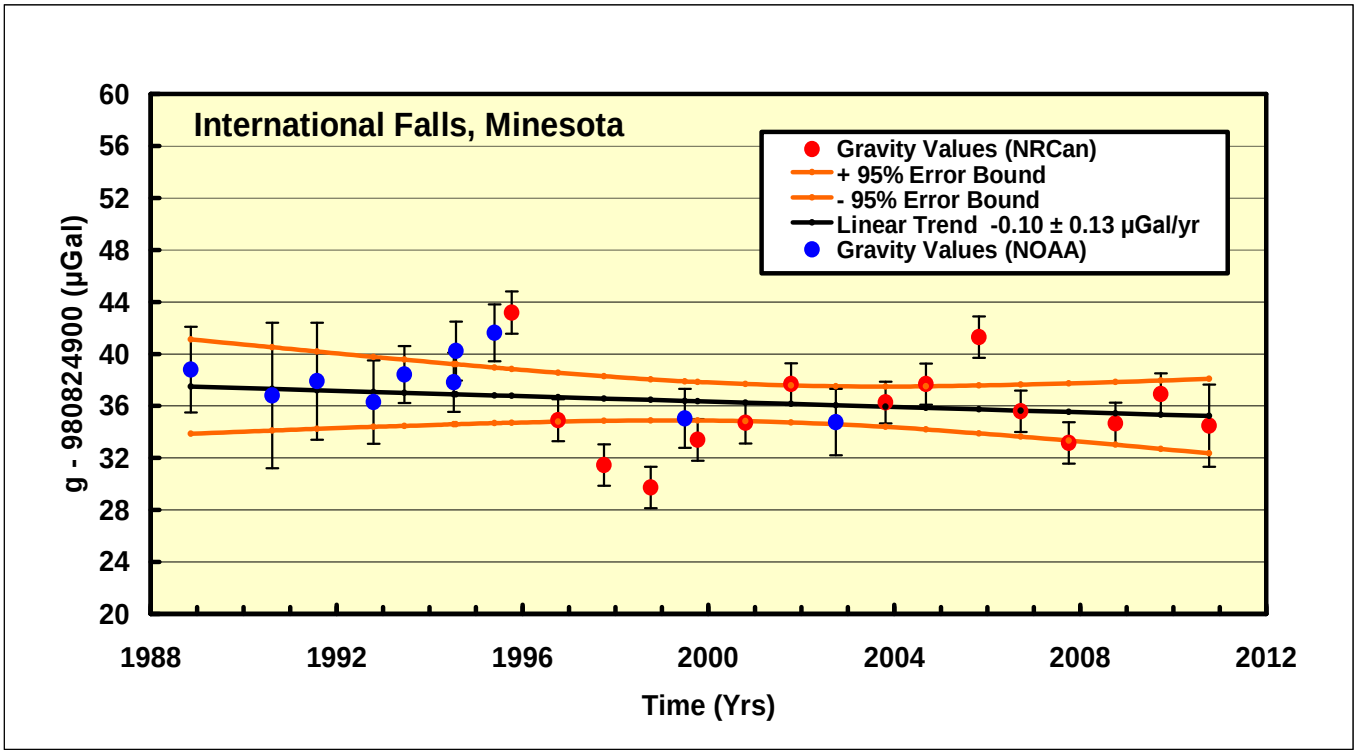

Figure 3d. Observed gravity at International Falls, Minnesota. Error bars denote standard errors.

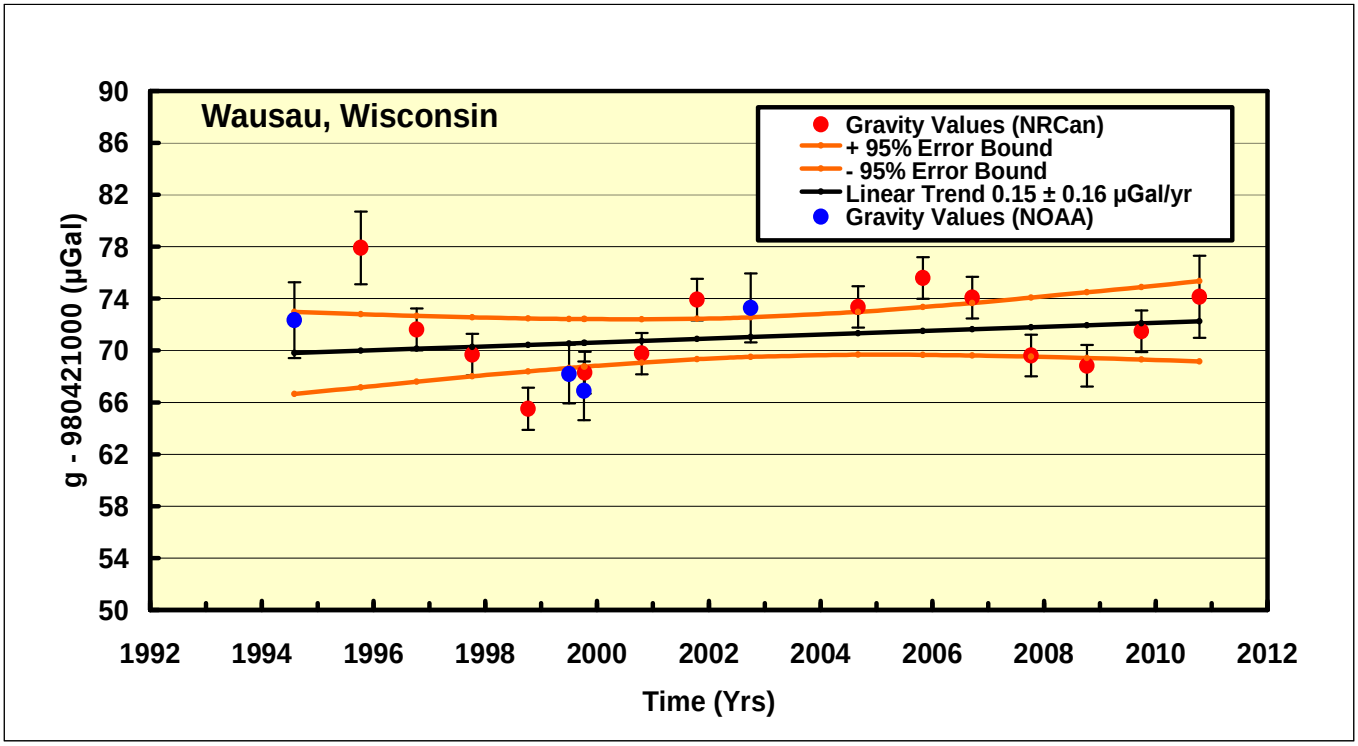

Figure 3e. Observed gravity at Wausau, Wisconsin. Error bars denote standard errors.

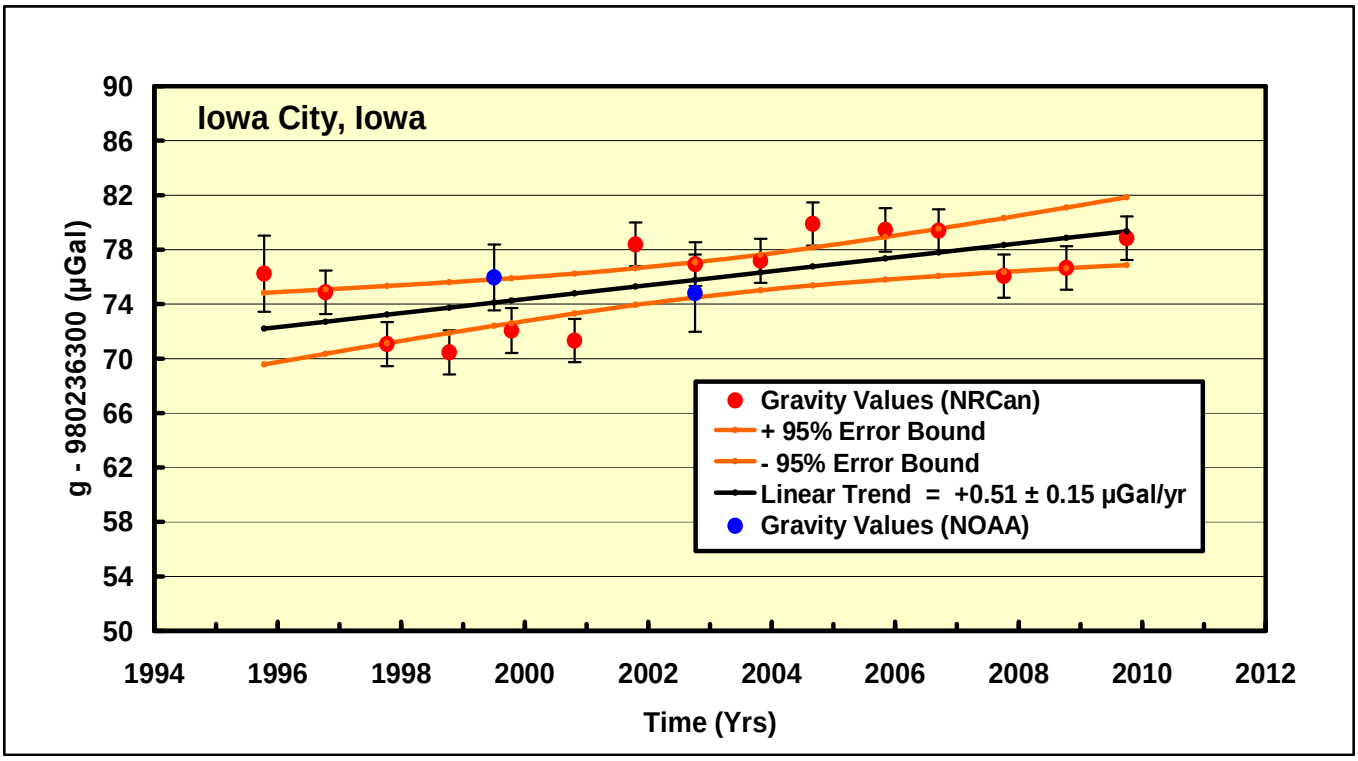

Figure 3f. Observed gravity at Iowa City, Iowa. Error bars denote standard errors.

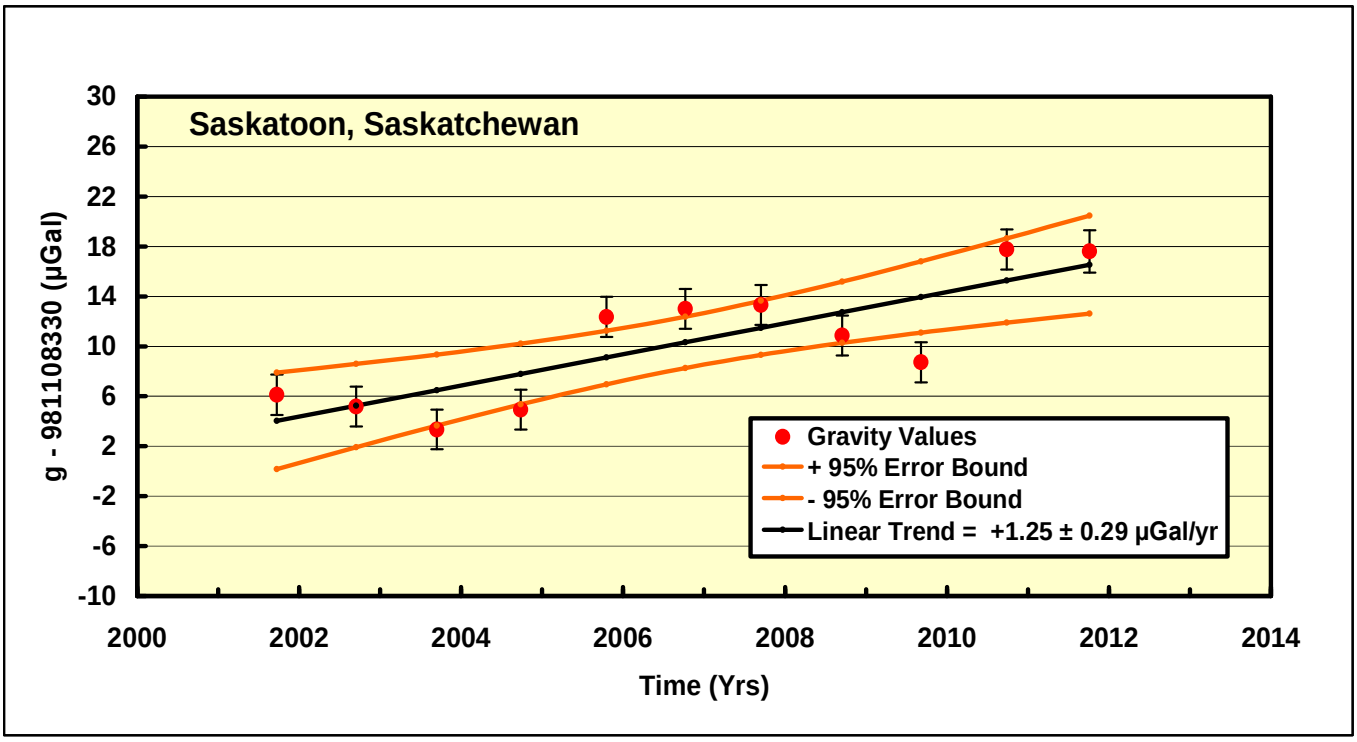

Figure 3g. Observed gravity at Saskatoon, Saskatchewan. Error bars denote standard errors.

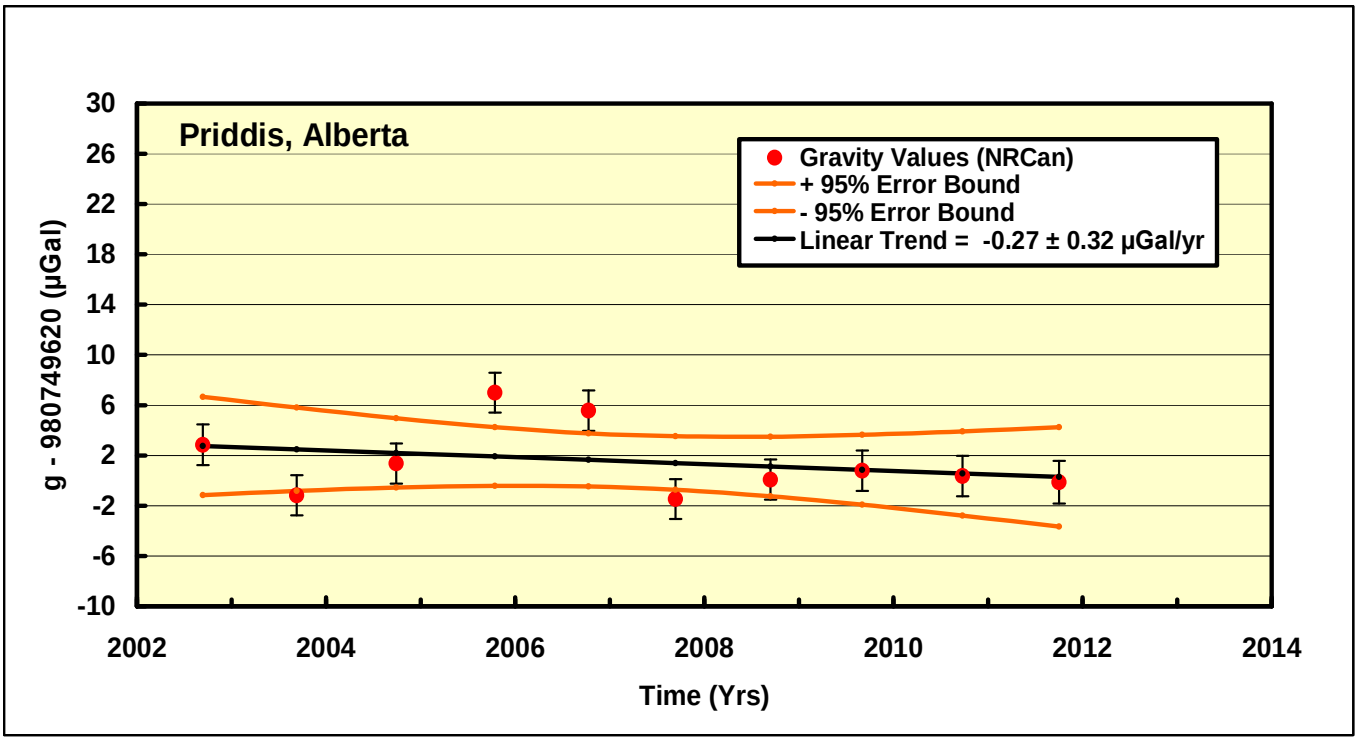

Figure 3h. Observed gravity at Priddis, Alberta. Error bars denote standard errors.

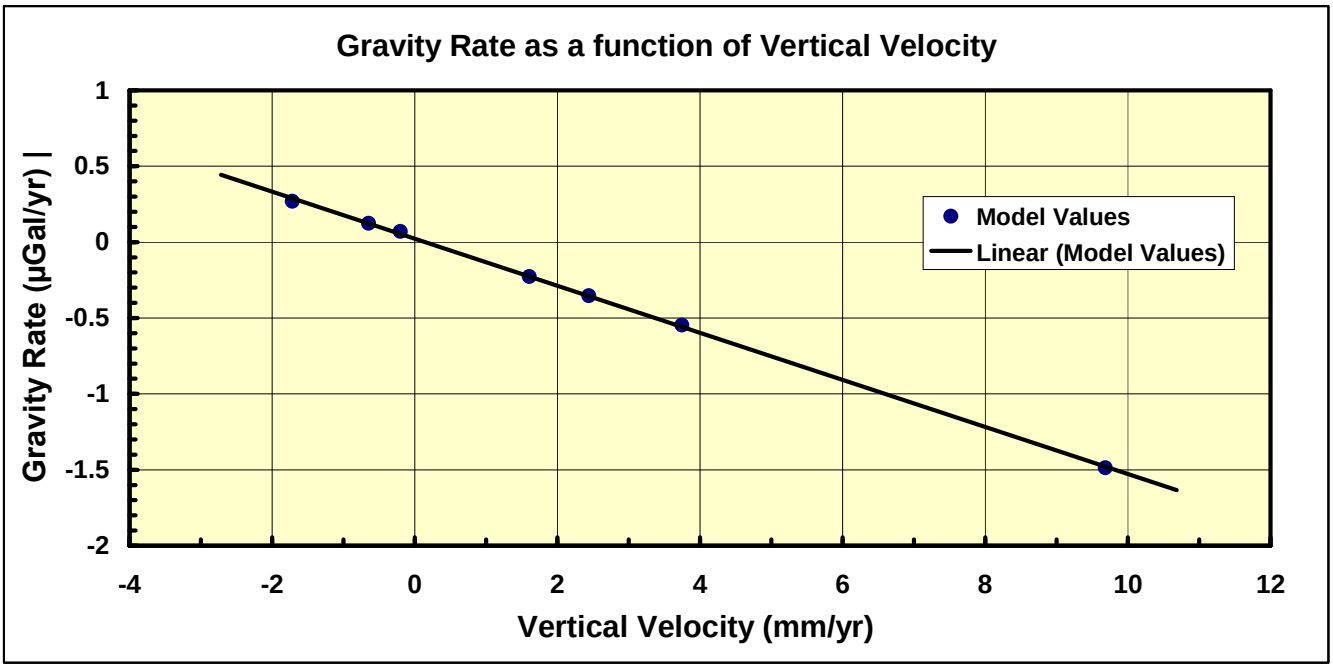

Figure 4. Theoretical values of vertical velocity and gravity rate for the seven observation sites used in the regression of Fig. 5, based on a preferred Laurentide ice sheet model and Earth viscosity structure known as MultiDome1.

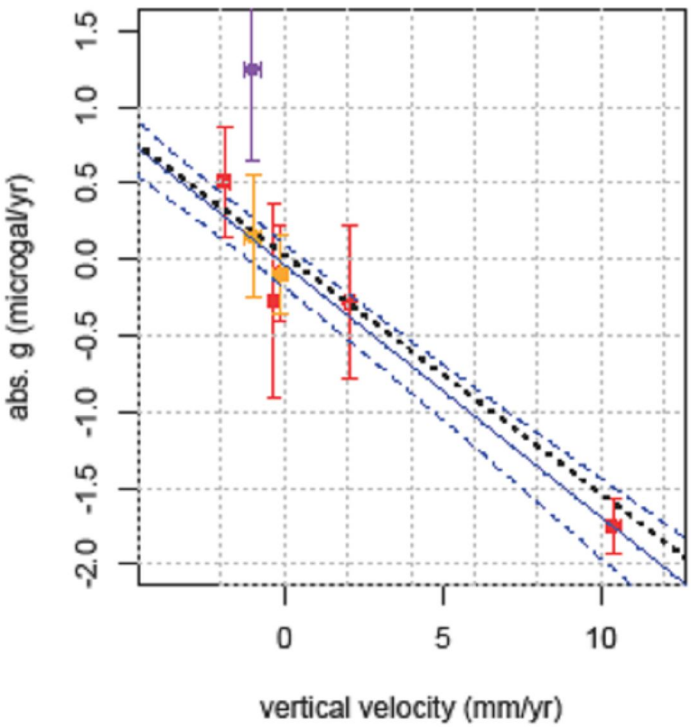

Figure 5. Absolute gravity vs. uplift rates. Red and orange symbols show absolute gravity and uplift rates with 95% confidence intervals at collocated and interpolated sites, respectively (cf. Table 1). Purple symbol shows absolute gravity and uplift rates at Saskatoon station (not used in fit). Blue solid and dashed lines show best-fit linear regression and its 95% confidence interval, respectively. Black dashed line shows model-predicted linear relation for reference.

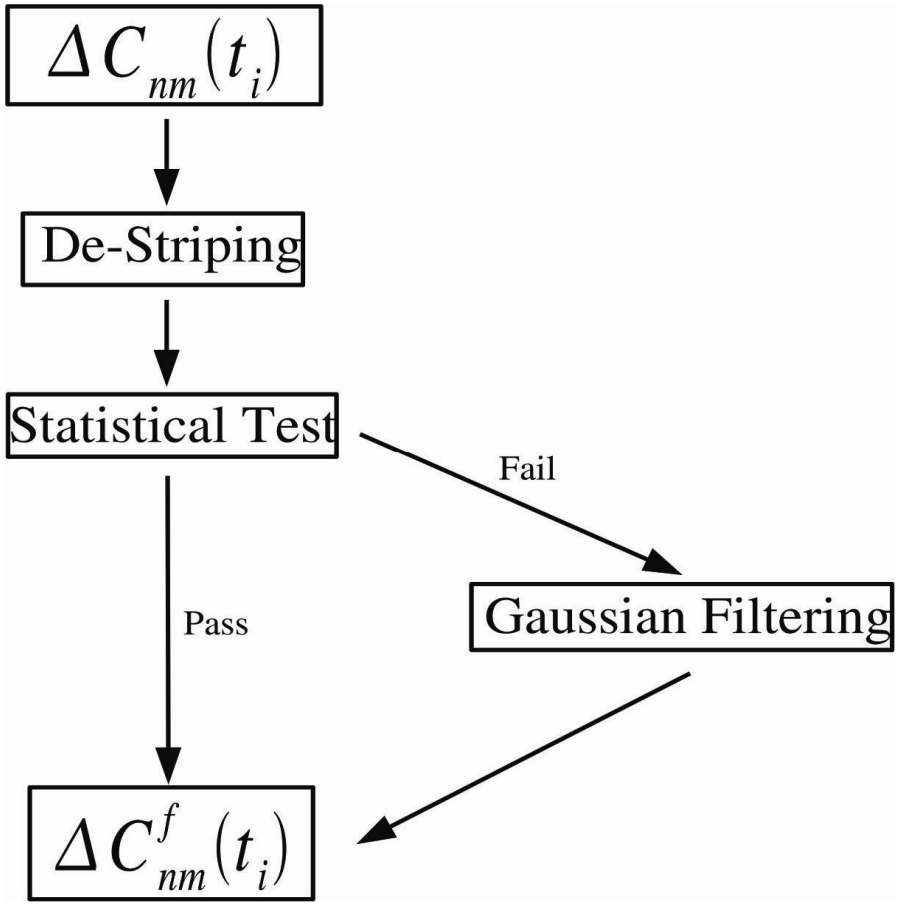

Figure 6. Flowchart of the two-step method for processing the monthly GRACE gravity models.

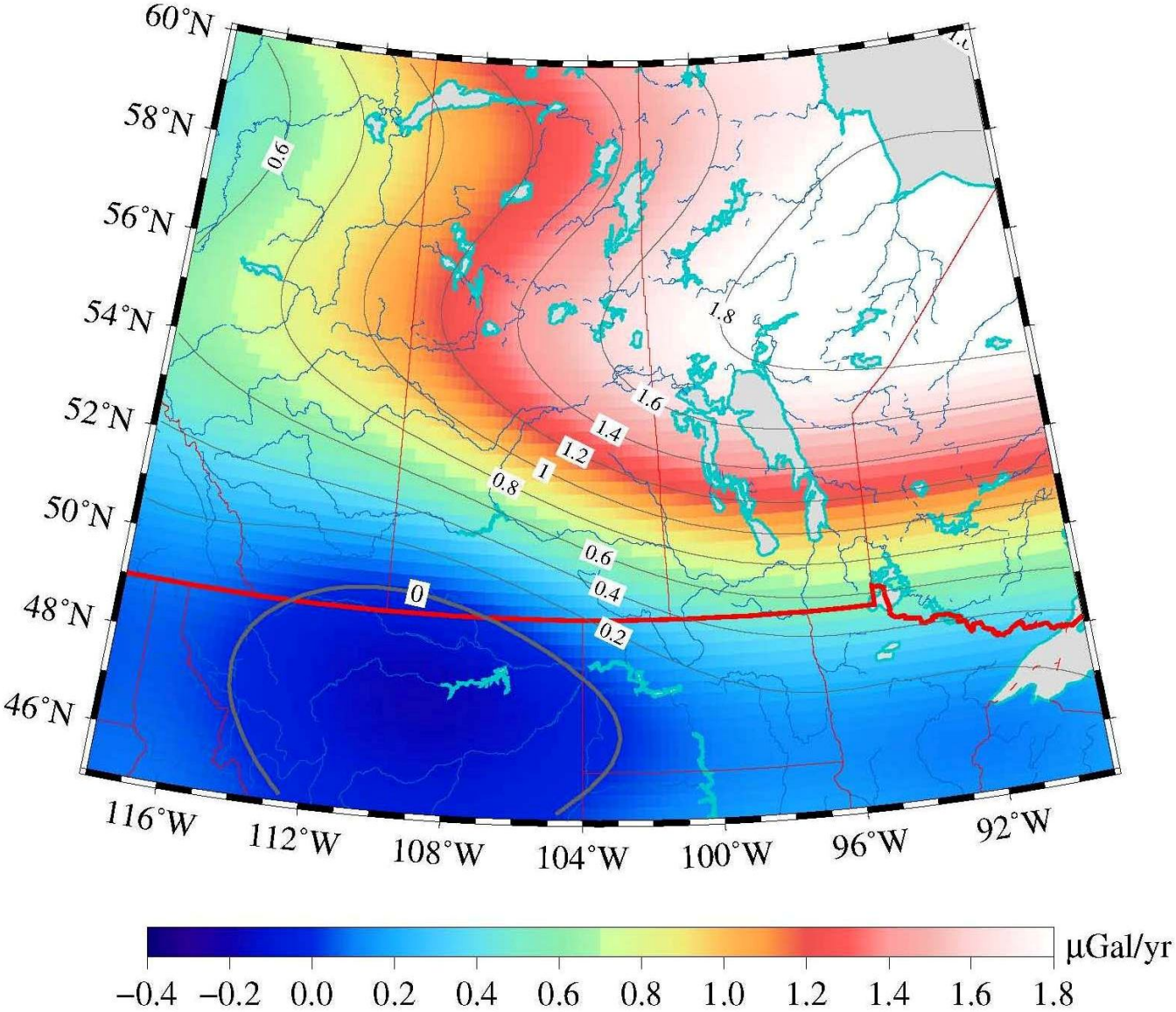

Figure 7. GRACE gravity change rate map based on 90 GRACE monthly gravity models.

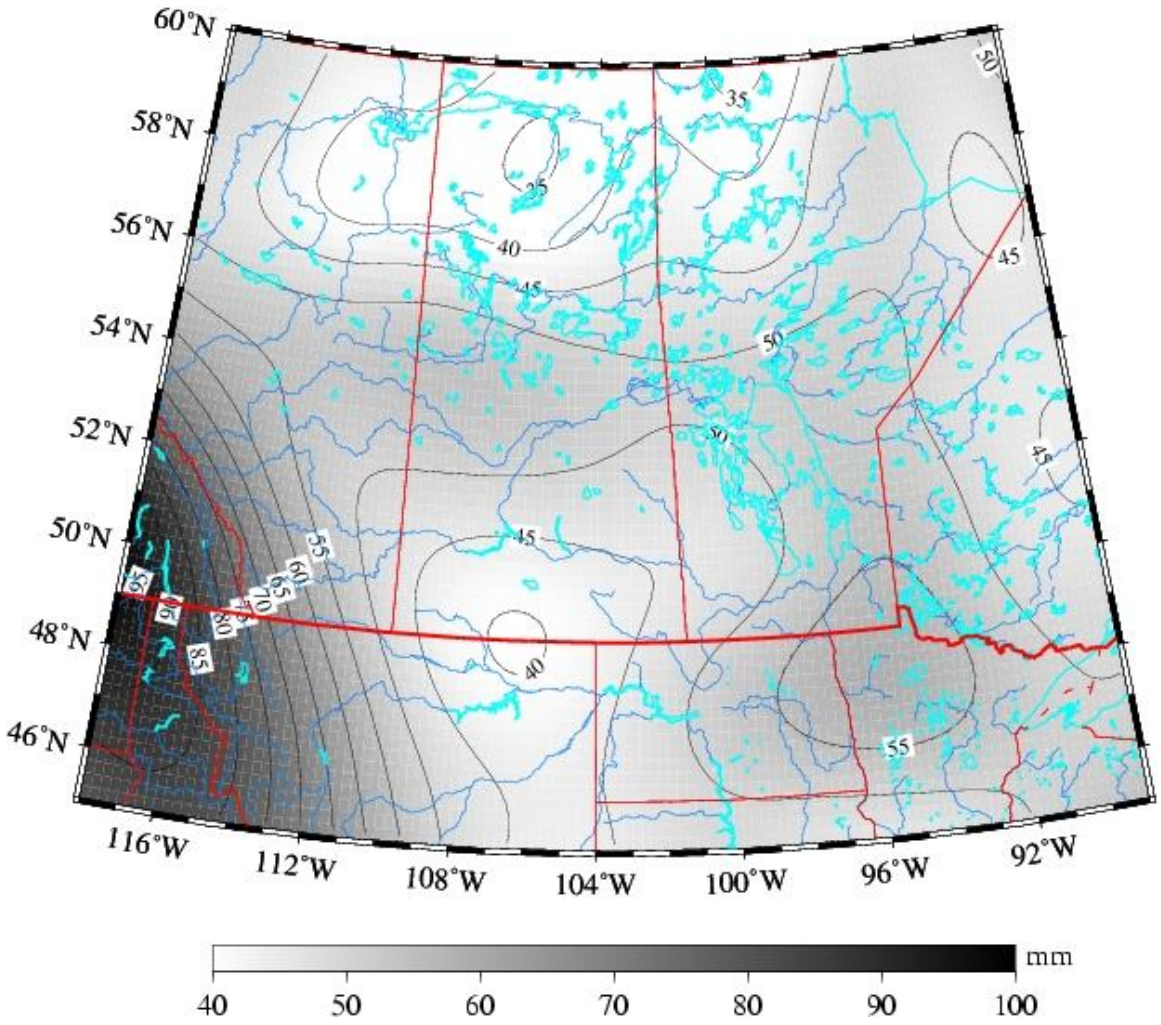

Figure 8. RMS variation of total water storage change in Water-Thickness-Equivalent after removing a linear trend over time from 90 monthly GRACE solutions.

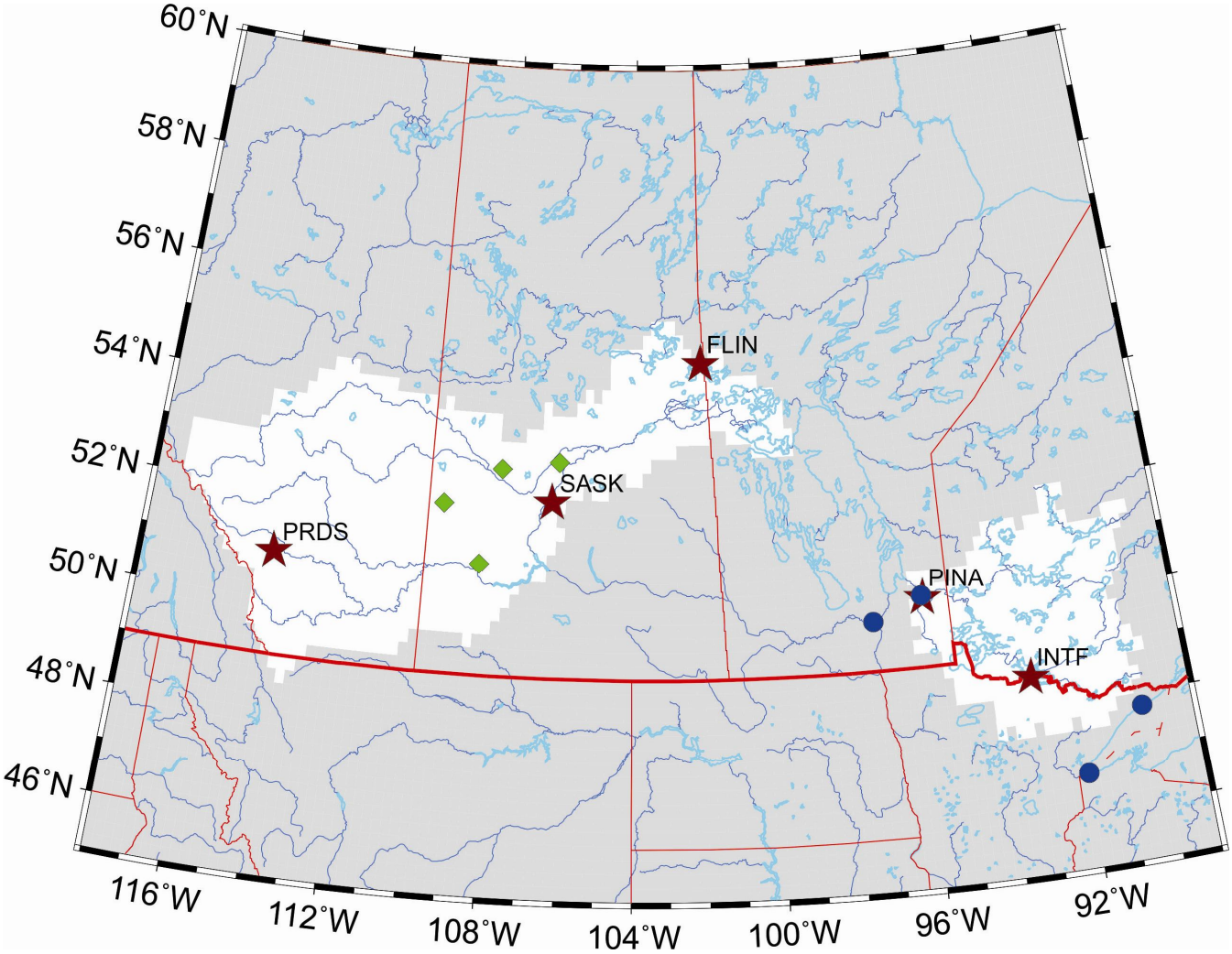

Figure 9. Saskatchewan River and Winnipeg River sub-basins. Red stars denote surface absolute gravity sites in the two basins. Blue dots denote GPS sites used to detect surface loading in the Winnipeg River sub-basin. Green diamonds denote deep observation wells near Saskatoon.

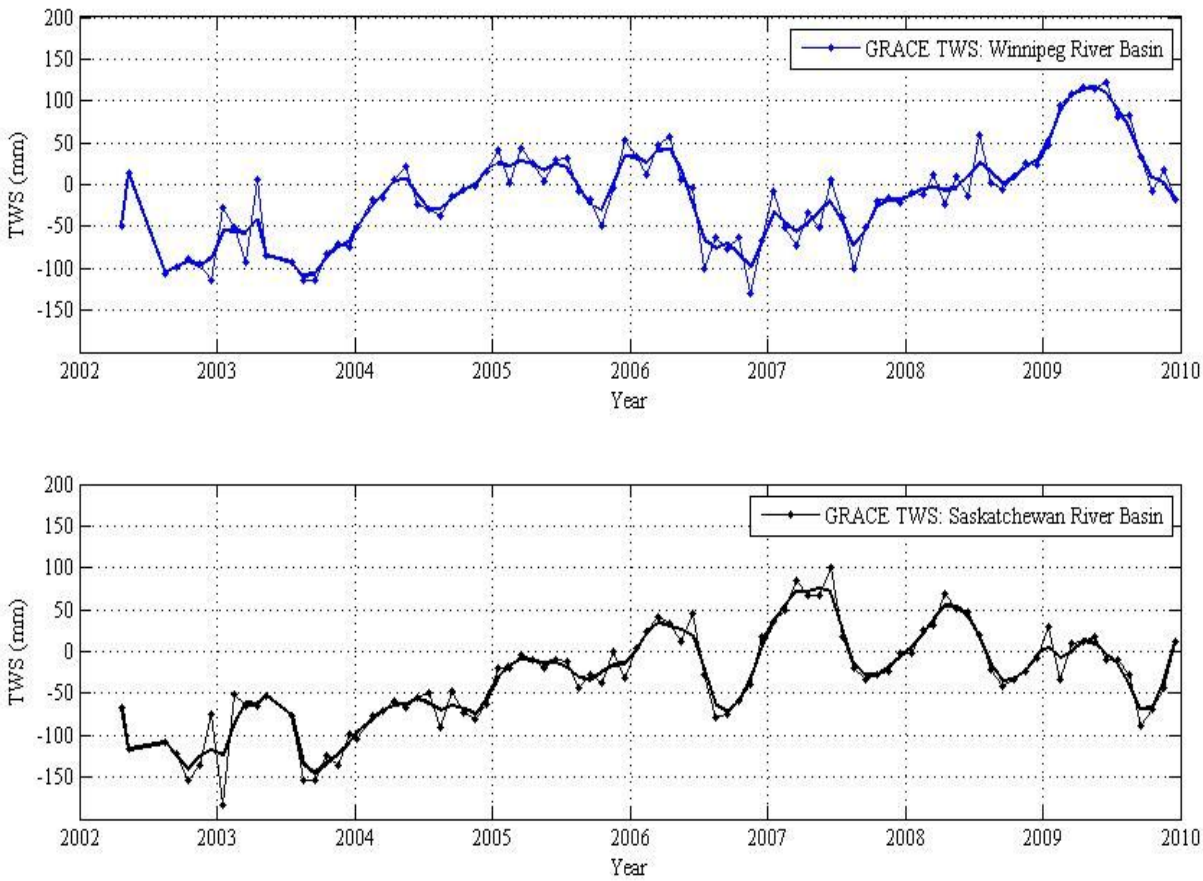

Figure 10. GRACE total water storage (TWS) changes over two water drainage basins shown in Fig. 9 relative to the mean over the period 2005 to 2009.

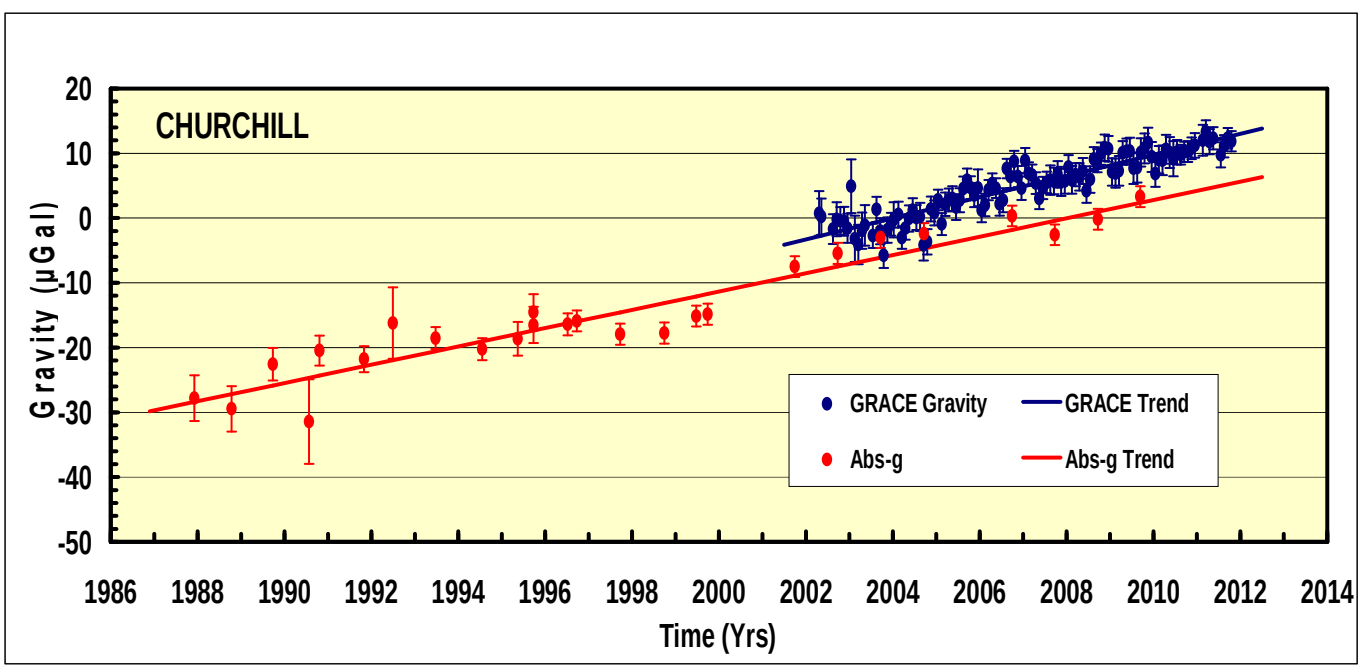

Figure 11a. Comparison of monthly GRACE gravity observations with surface absolute-g observations at Churchill, Manitoba corrected for the effect of vertical velocity using co-located GPS.

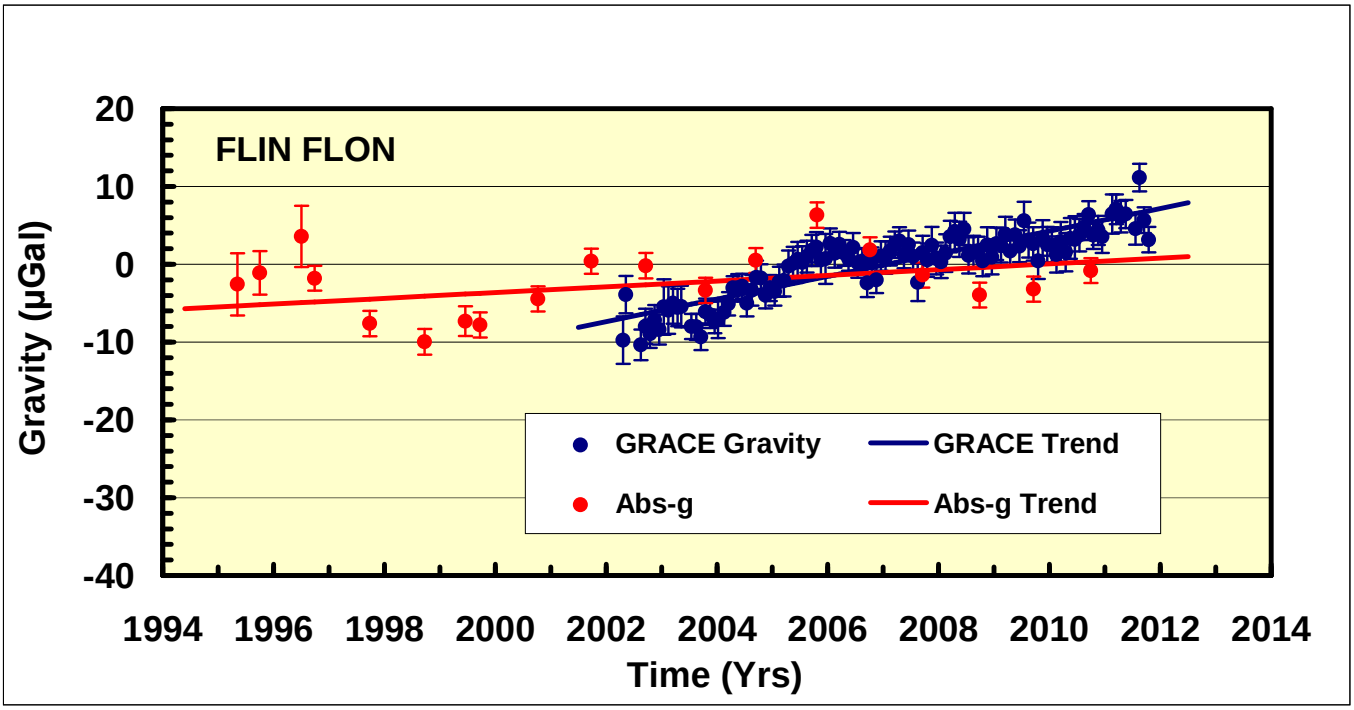

Figure 11b. Comparison of monthly GRACE gravity observations with surface absolute-g observations at Flin Flon, Manitoba corrected for the effect of vertical velocity using co-located GPS.

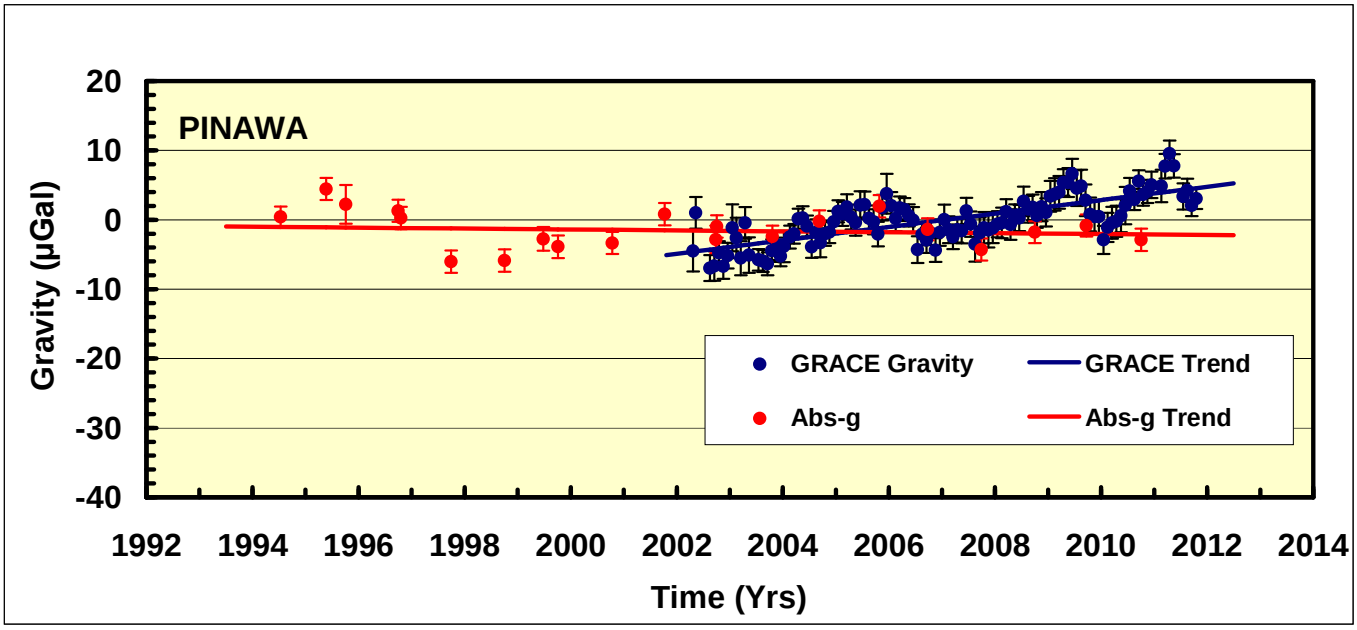

Figure 11c. Comparison of monthly GRACE gravity observations with surface absolute-g observations at Pinawa, Manitoba corrected for the effect of vertical velocity using co-located GPS.

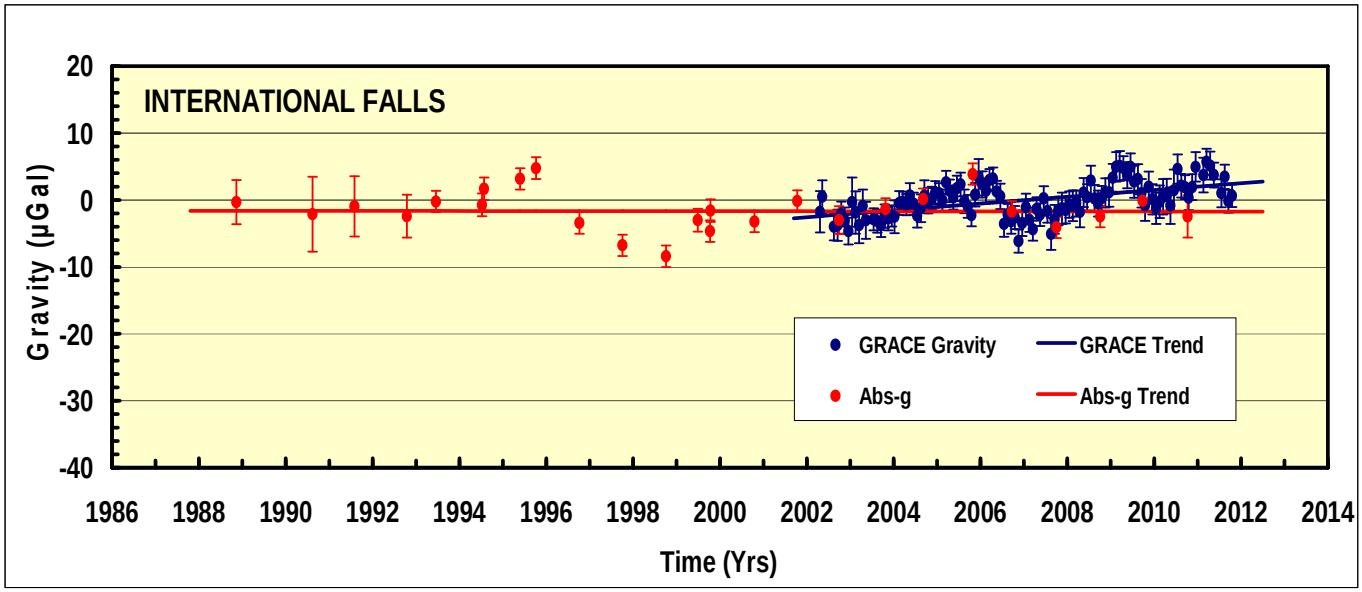

Figure 11d. Comparison of monthly GRACE gravity observations with surface absolute-g observations at International Falls, Minnesota corrected for the effect of vertical velocity using co-located GPS.

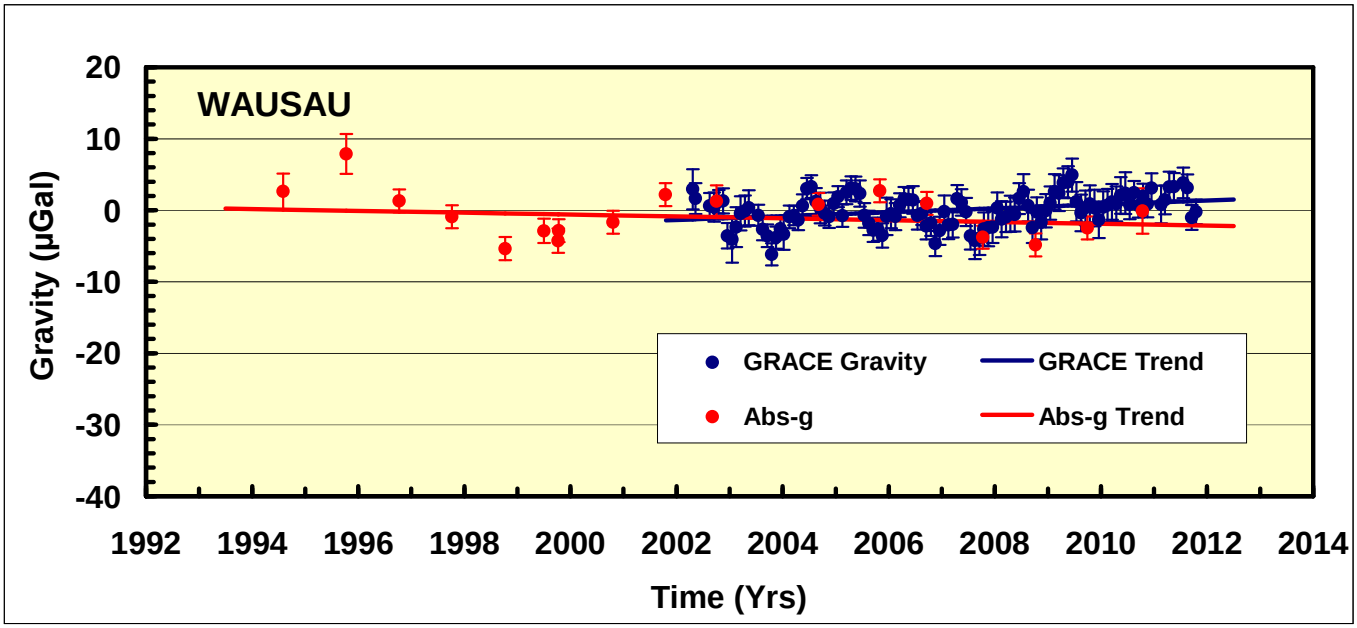

Figure 11e. Comparison of monthly GRACE gravity observations with surface absolute-g observations at Wausau, Wisconsin corrected for the effect of vertical velocity using co-located GPS.

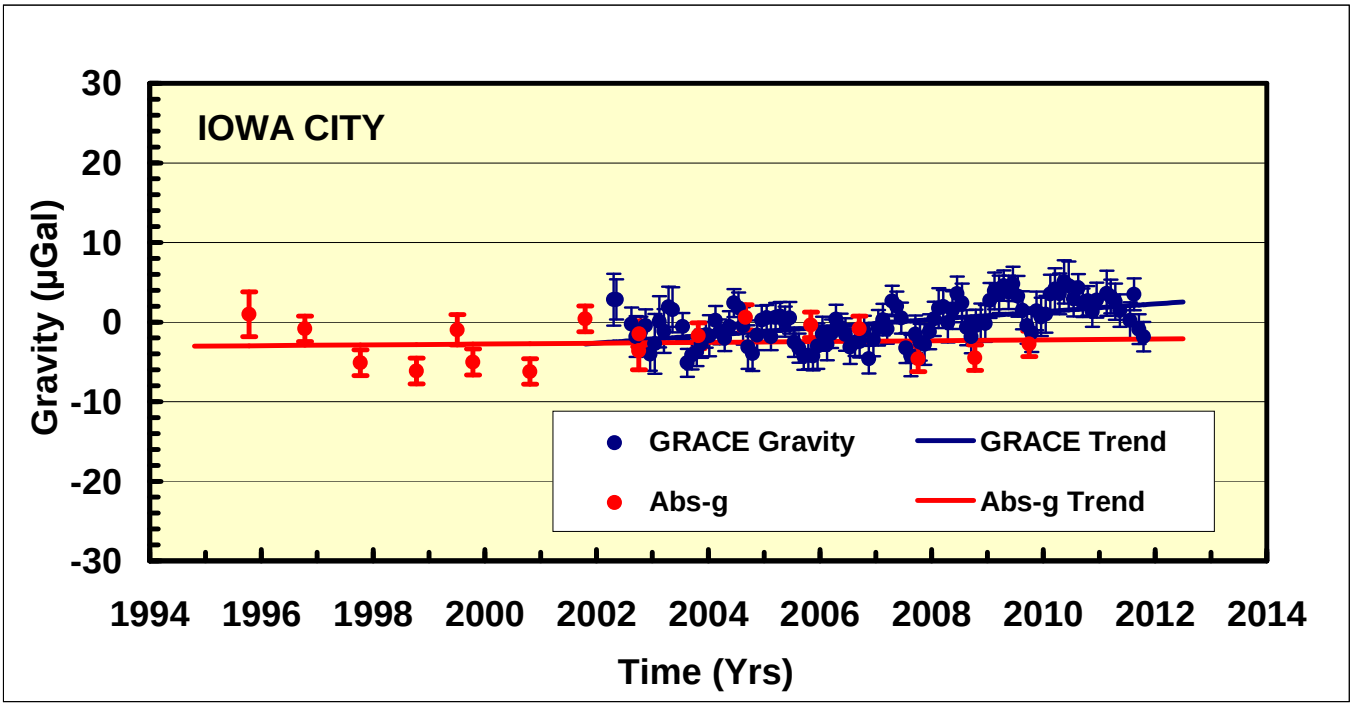

Figure 11f. Comparison of monthly GRACE gravity observations with surface absolute-g observations at Iowa City, Iowa corrected for the effect of vertical velocity using co-located GPS.

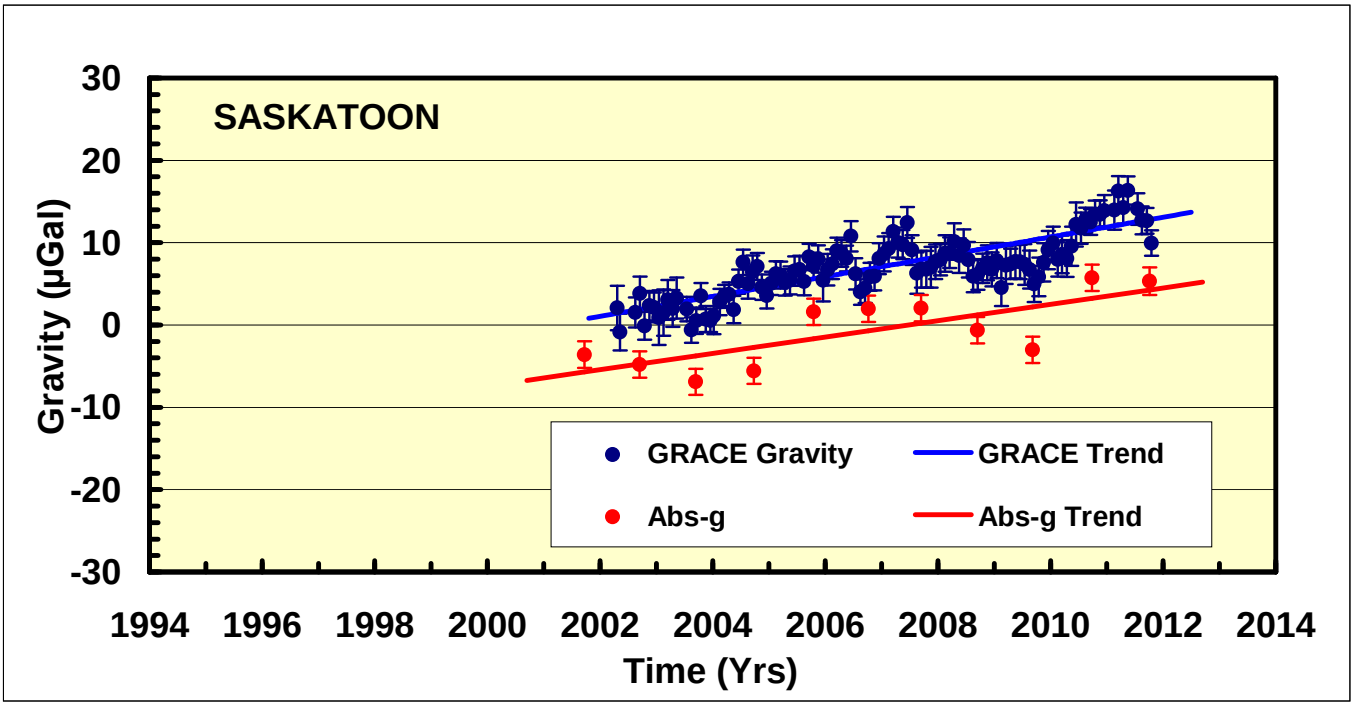

Figure 11g. Comparison of monthly GRACE gravity observations with surface absolute-g observations at Saskatoon, Saskatchewan corrected for the effect of vertical velocity using co-located GPS.

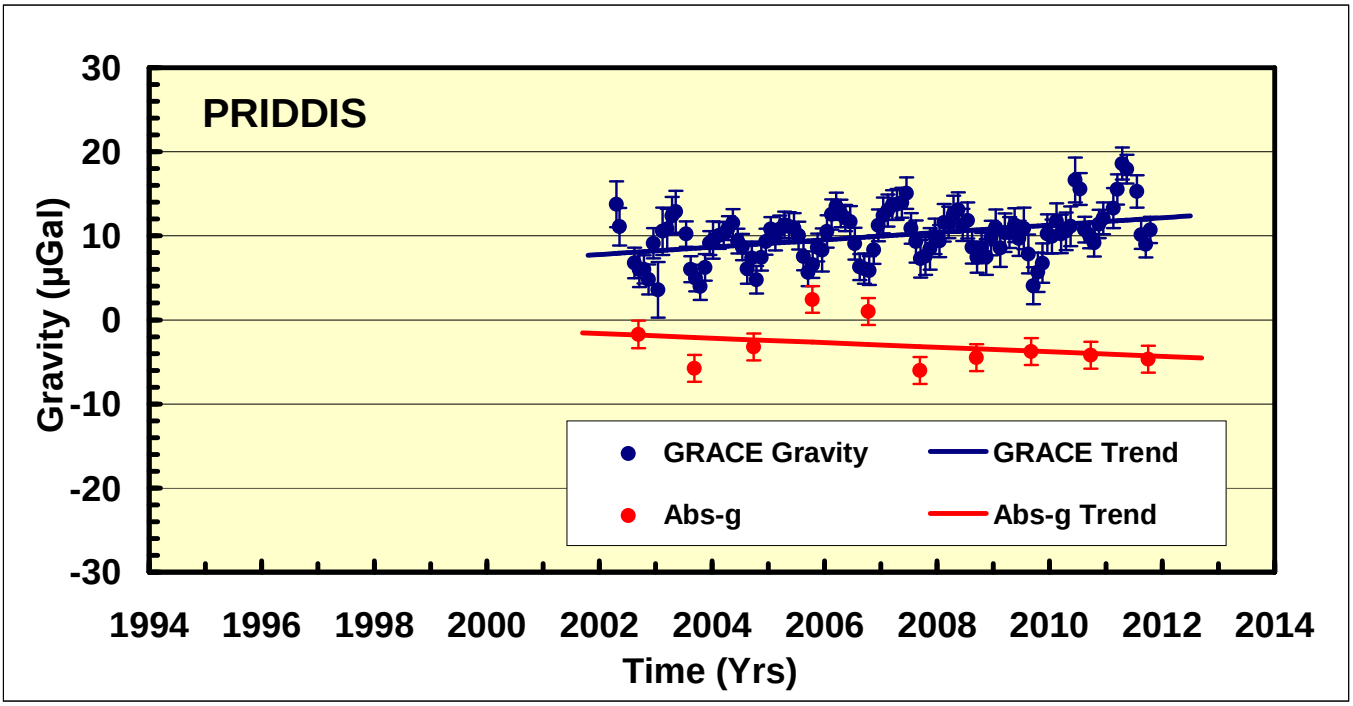

Figure 11h. Comparison of monthly GRACE gravity observations with surface absolute-g observations at Priddis, Alberta corrected for the effect of vertical velocity using co-located GPS.

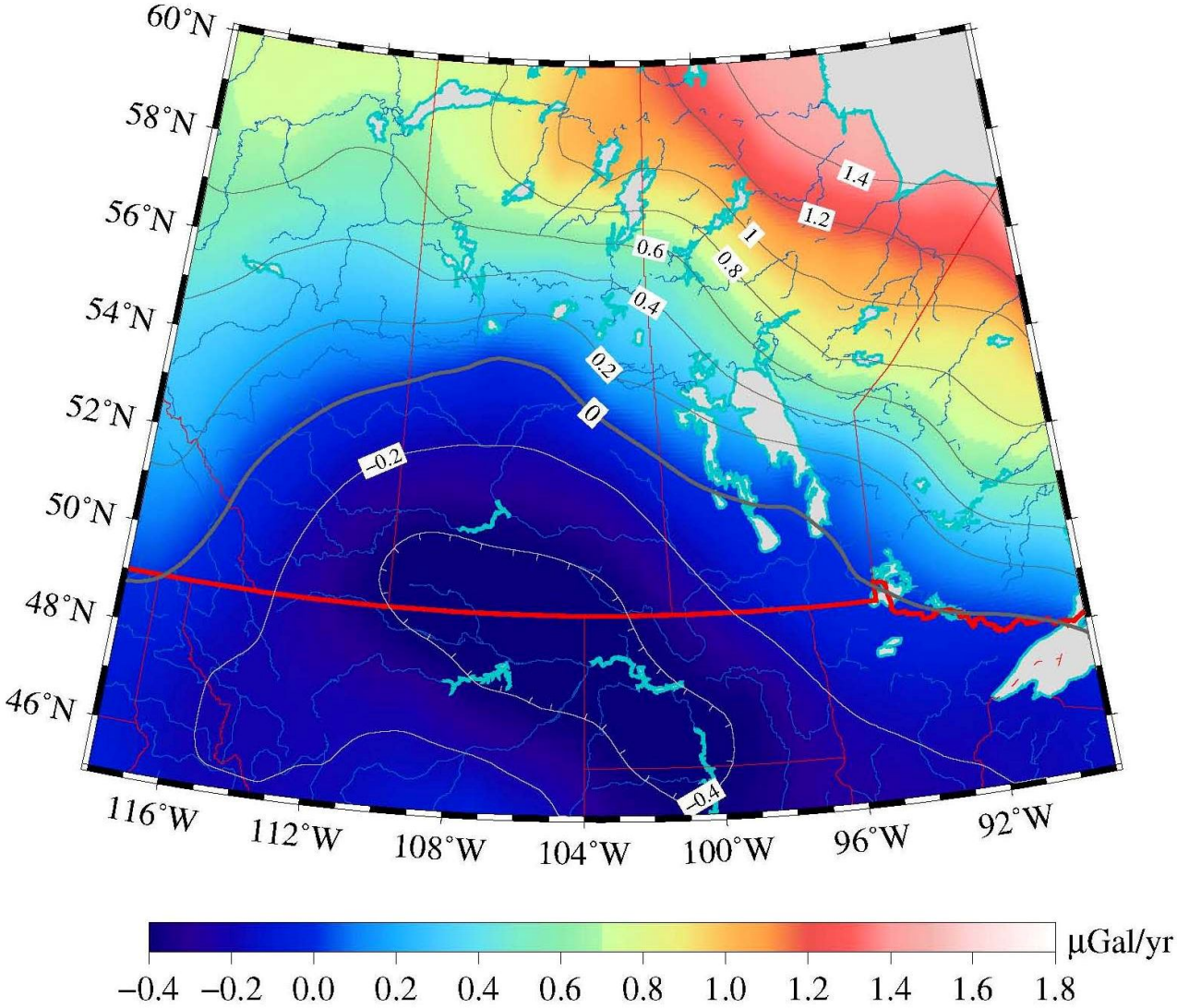

Figure 12. Gravity mass re-distribution rate map for the Nelson River drainage basin derived from Fig. 2 using the relation between surface gravity rates and GPS vertical rates established in section 4.3

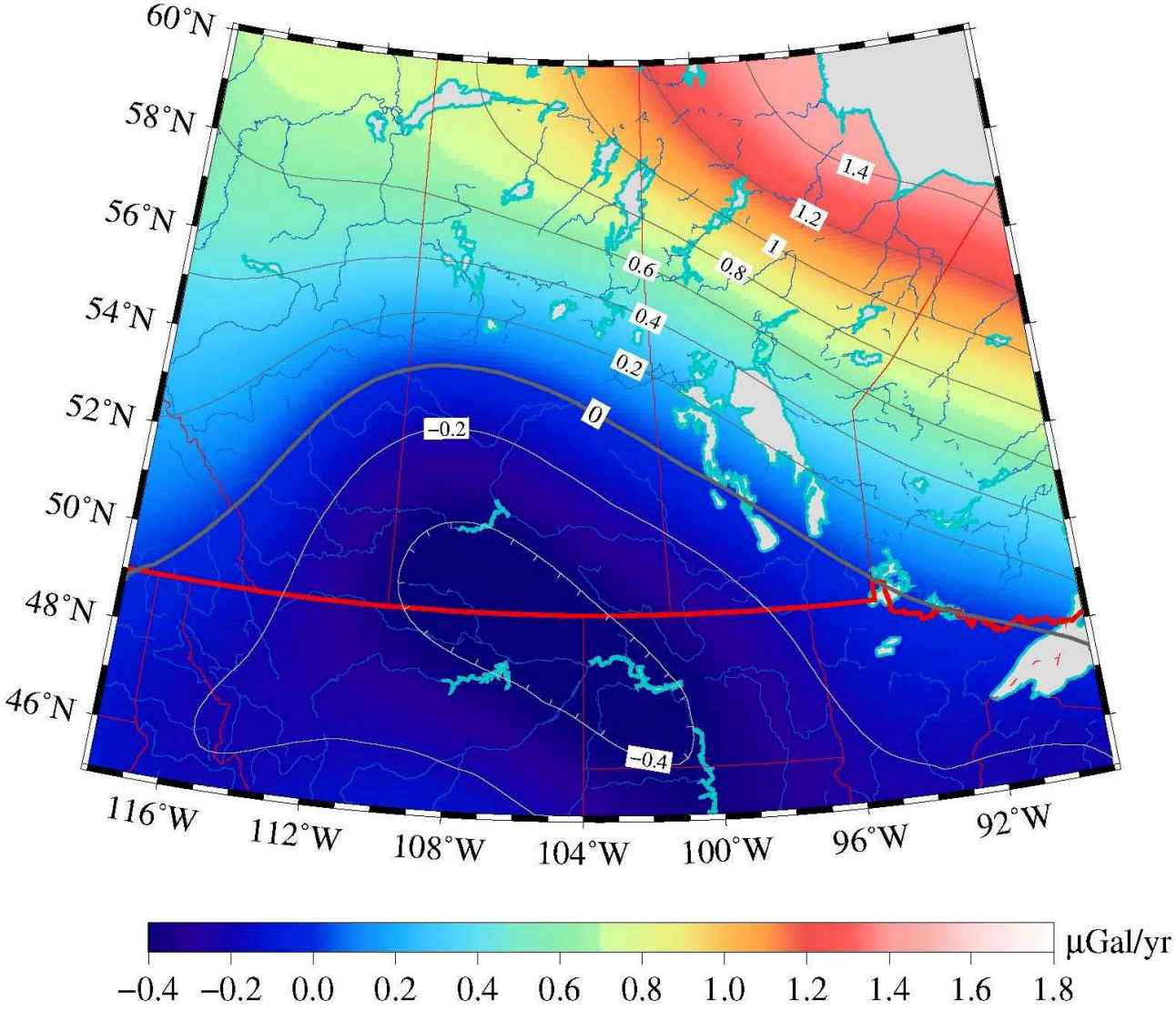

Figure 13. Gravity mass re-distribution rate map of Fig. 12 expressed in spherical harmonics truncated at degree and order 60.

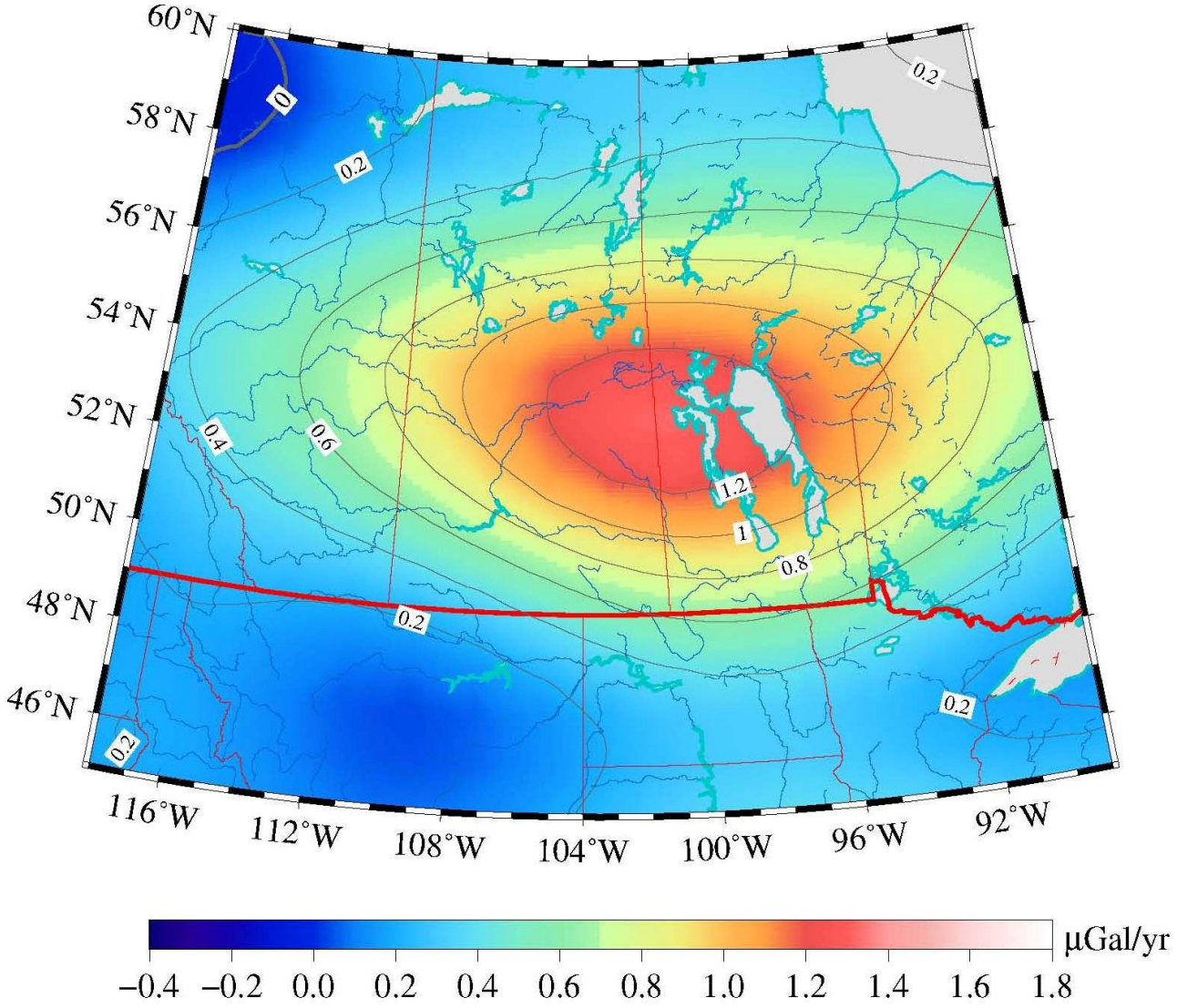

Figure 14. Map of difference in gravity rate between GRACE and 'virtual' gravity rates derived from GPS vertical rates (Fig.7 minus Fig. 13).

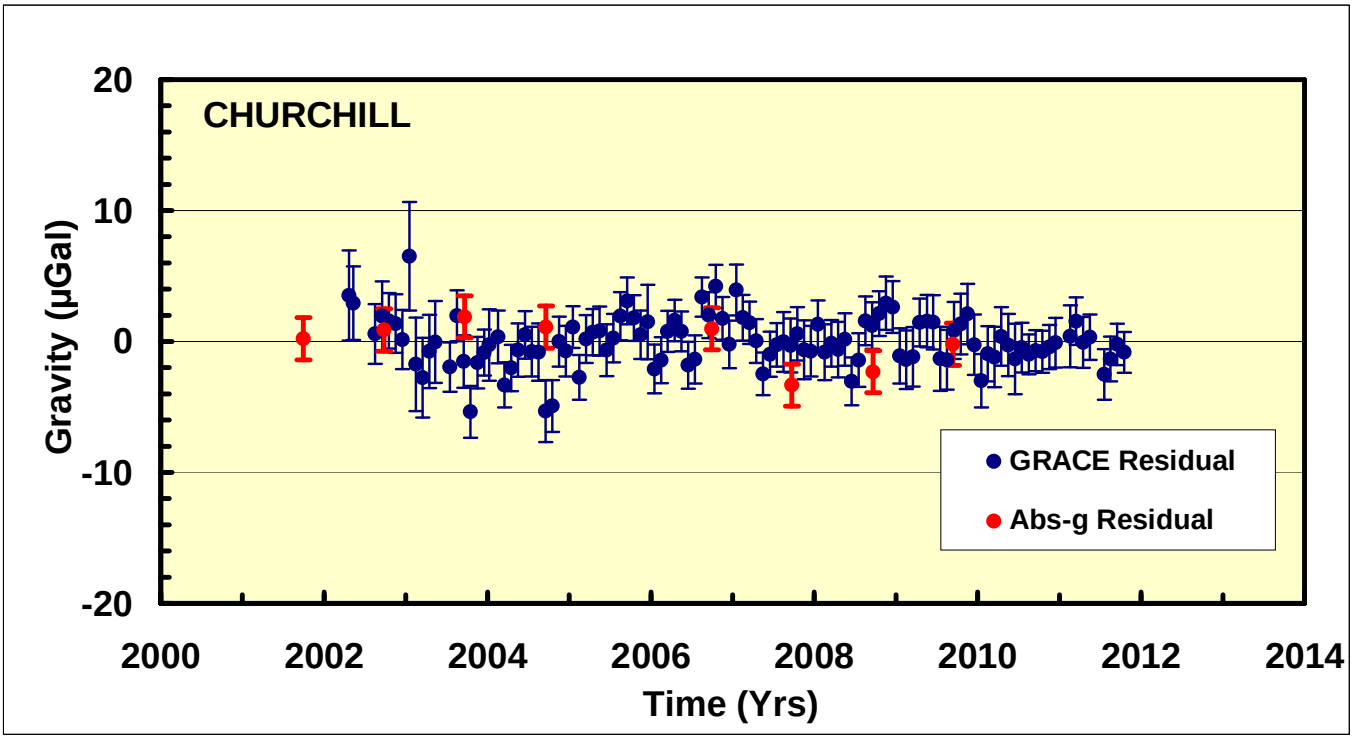

Figure 15a. Comparison of inter-annual variations between GRACE and surface gravity at Churchill, Manitoba.

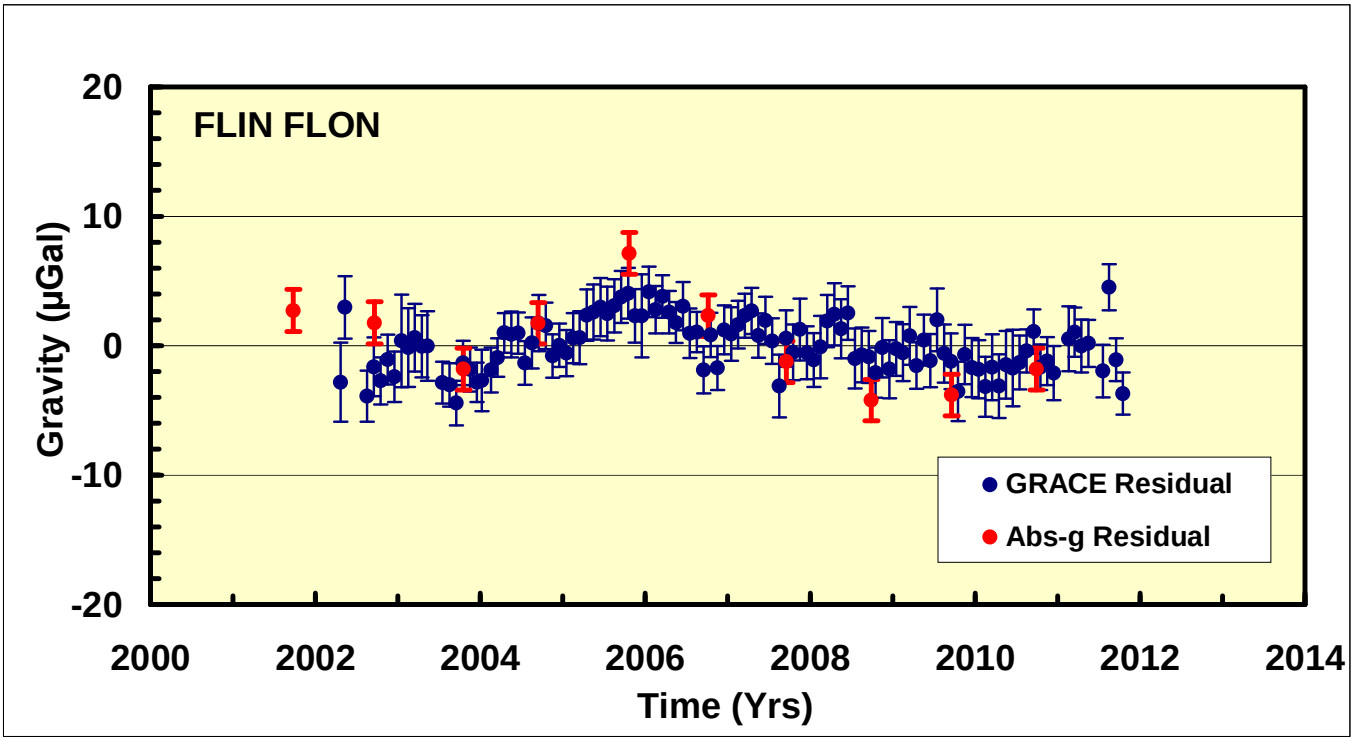

Figure 15b. Comparison of inter-annual variations between GRACE and surface gravity at Flin Flon, Manitoba.

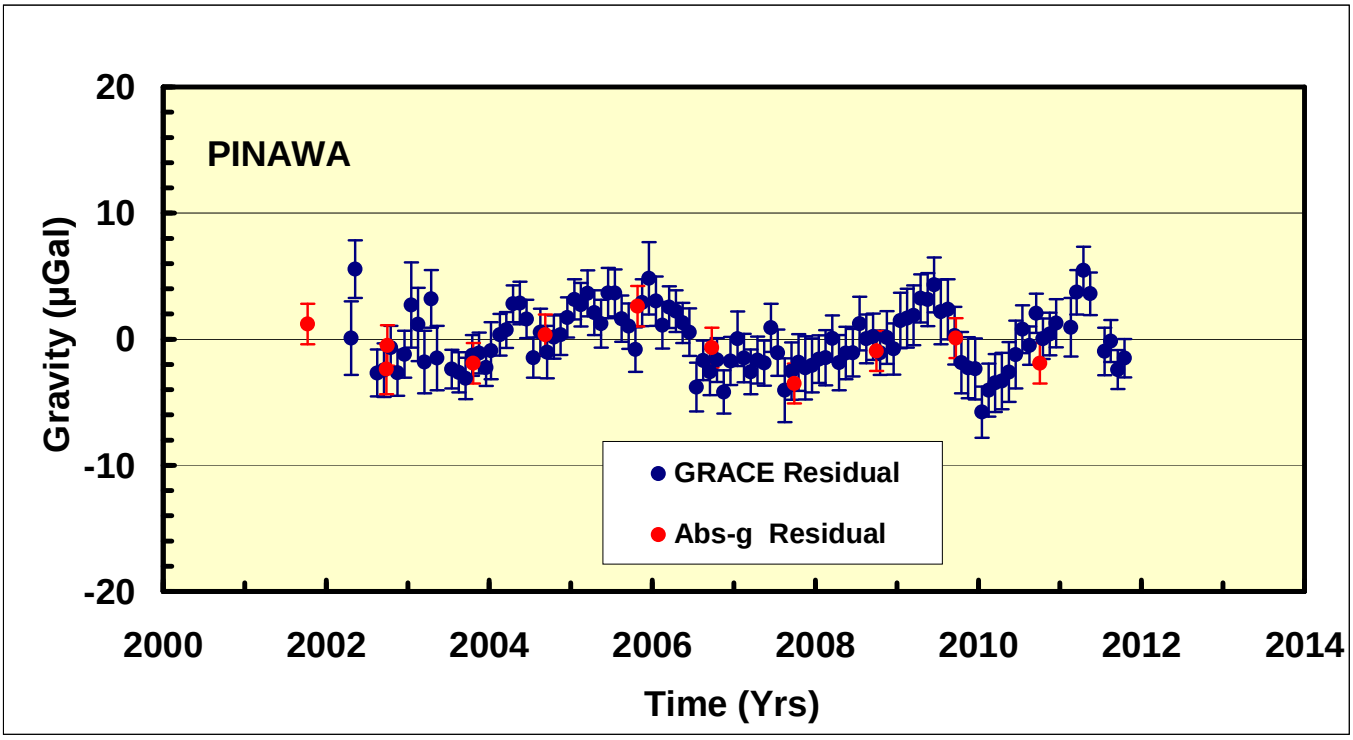

Figure 15c. Comparison of inter-annual variations between GRACE and surface gravity at Pinawa, Manitoba.

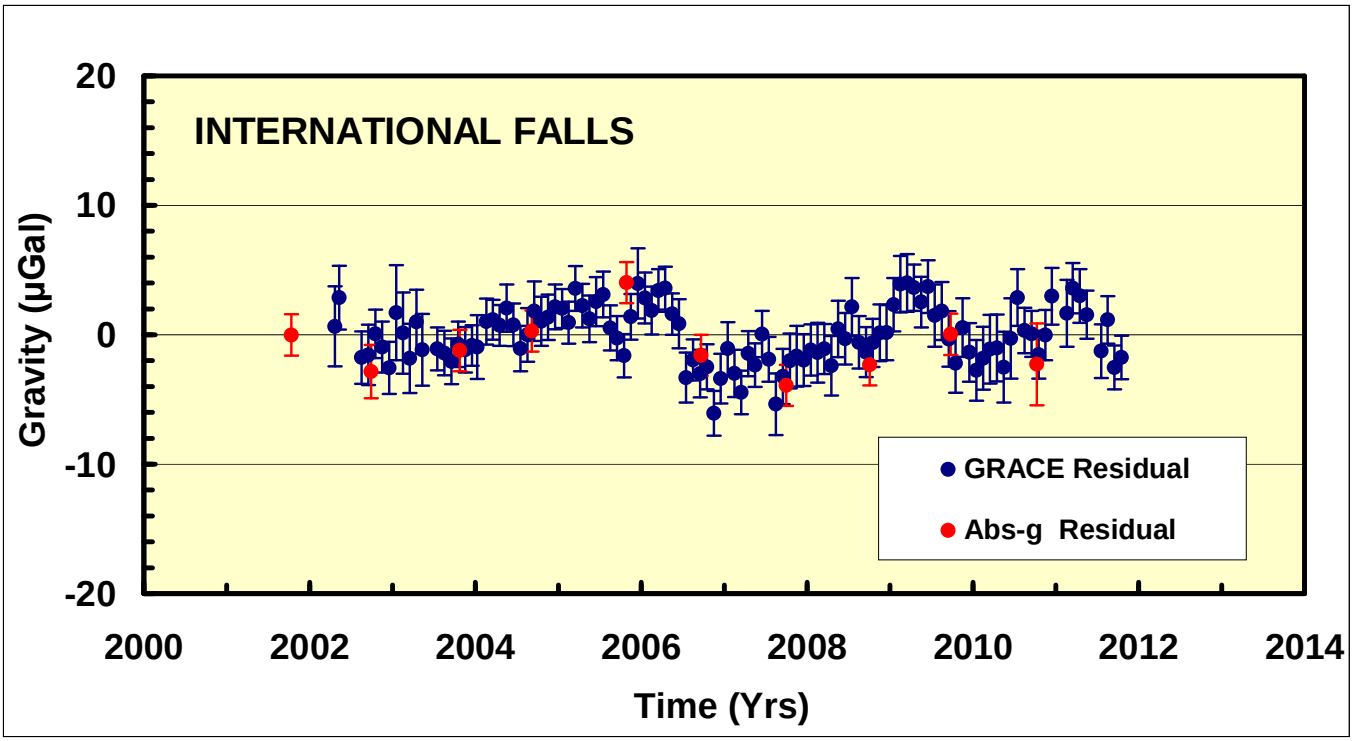

Figure 15d. Comparison of inter-annual variations between GRACE and surface gravity at International Falls, Minnesota.

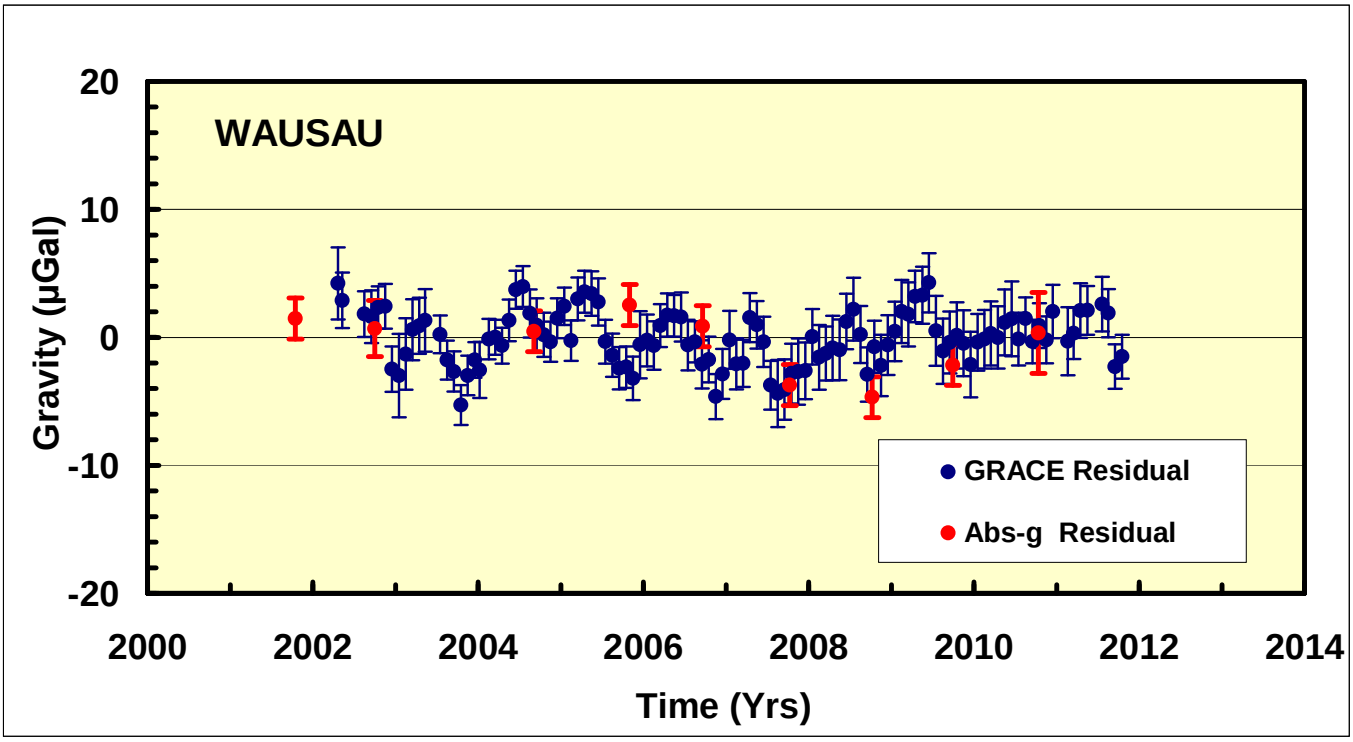

Figure 15e. Comparison of inter-annual variations between GRACE and surface gravity at Wausau, Wisconsin.

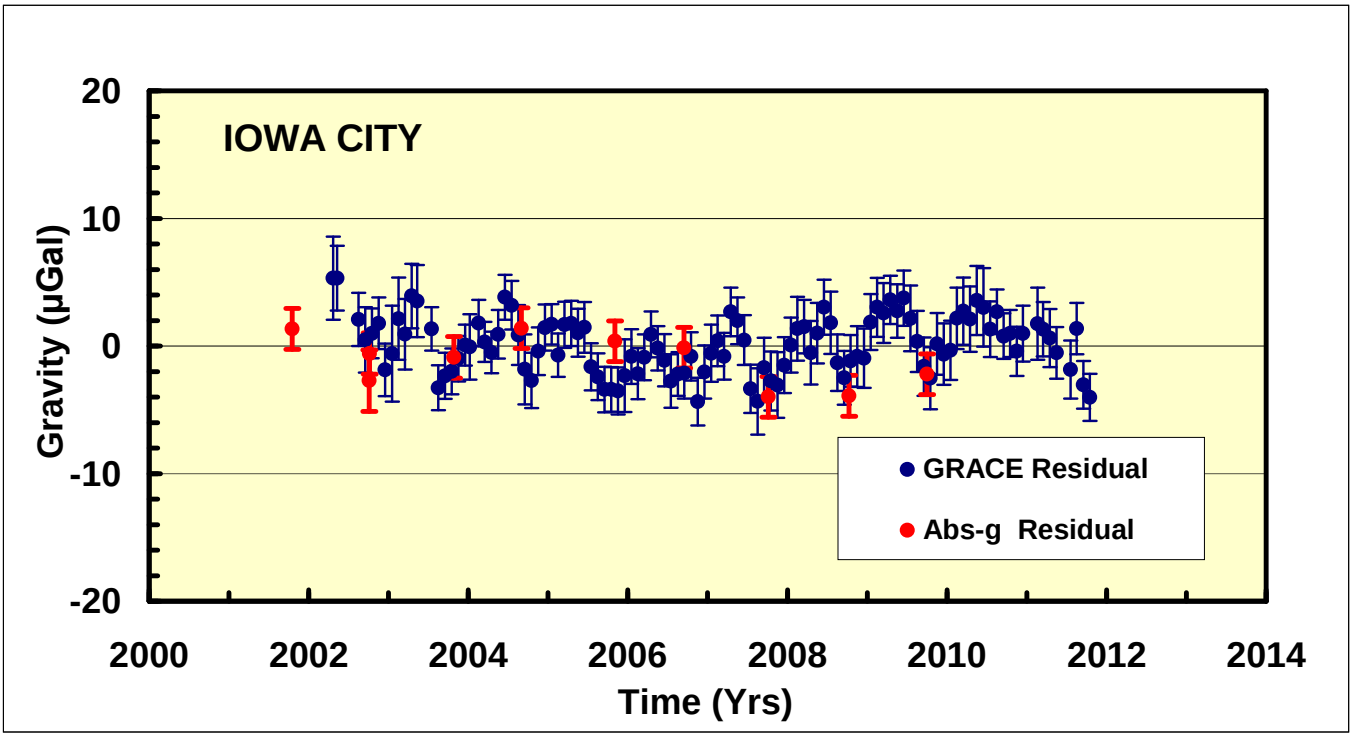

Figure 15f. Comparison of inter-annual variations between GRACE and surface gravity at Iowa City, Iowa.

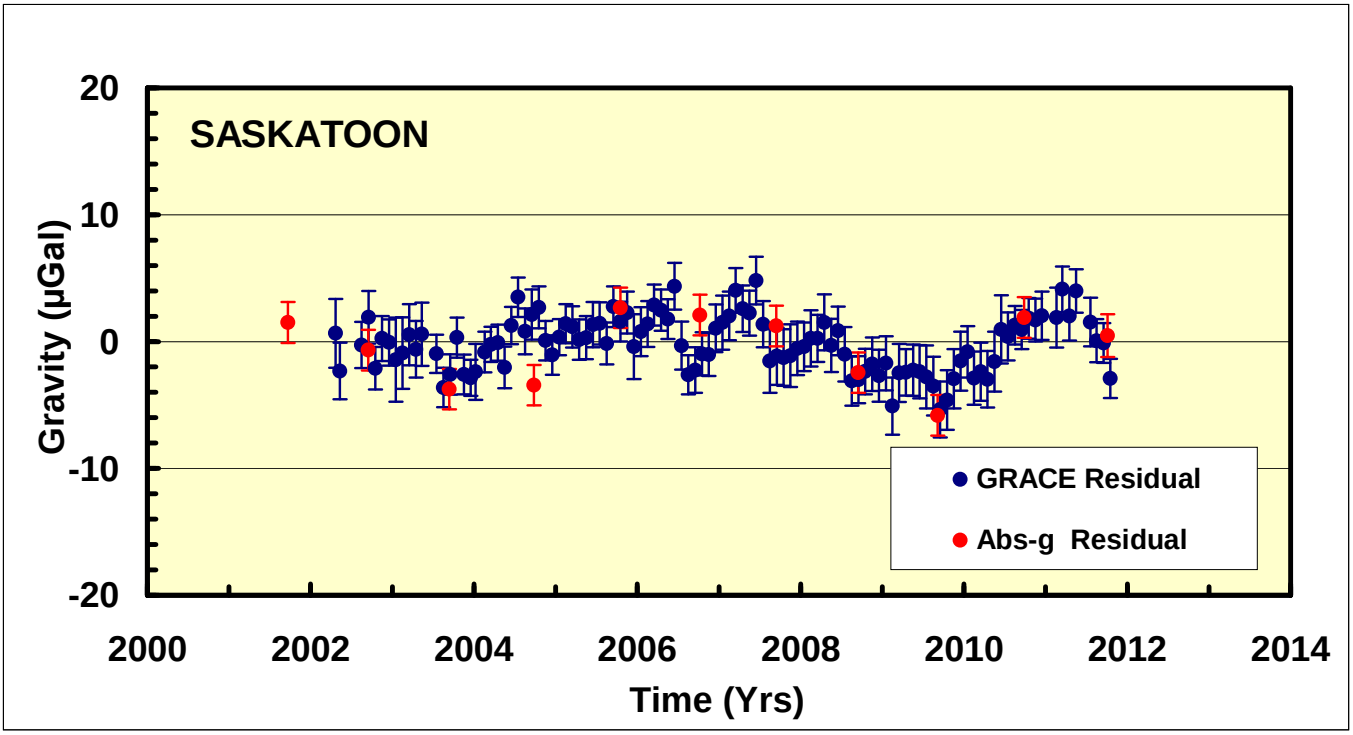

Figure 15g. Comparison of inter-annual variations between GRACE and surface gravity at Saskatoon, Saskatchewan.

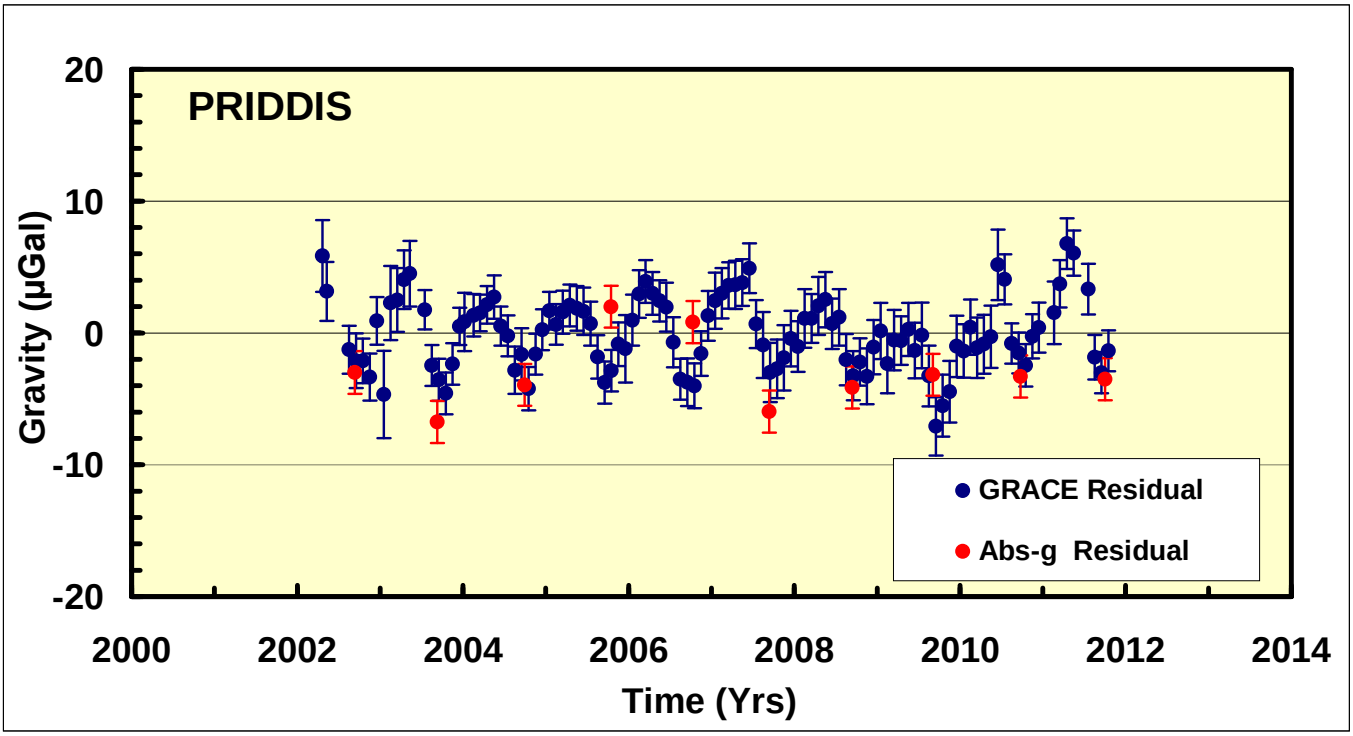

Figure 15h. Comparison of inter-annual variations between GRACE and surface gravity at Priddis, Alberta.

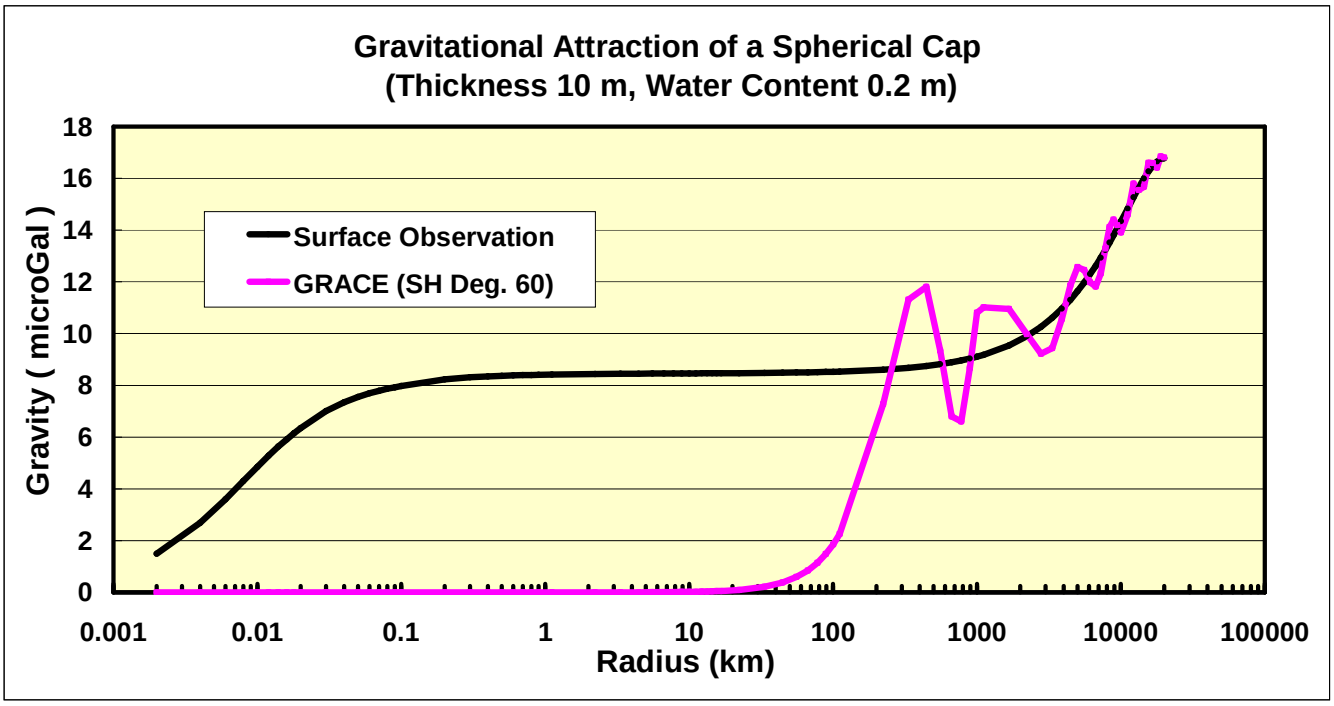

Figure 16. Comparison of the response of a surface gravity observation and a GRACE observation to a spherical cap of different radii on the Earth's surface. Ocillations in the GRACE response are the result of spherical harmonic truncation error in the absence of filtering.

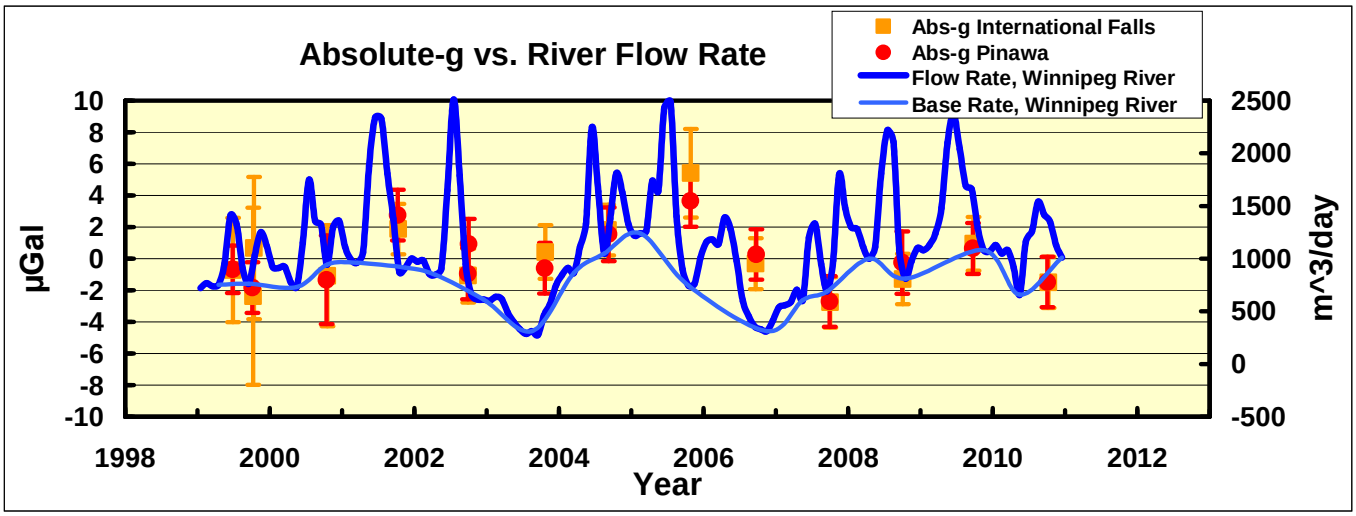

Figure 17a. Absolute gravity observations at International Falls, Minnesota and Pinawa, Manitoba compared to flow rates at Pine Falls on the Winnipeg River.

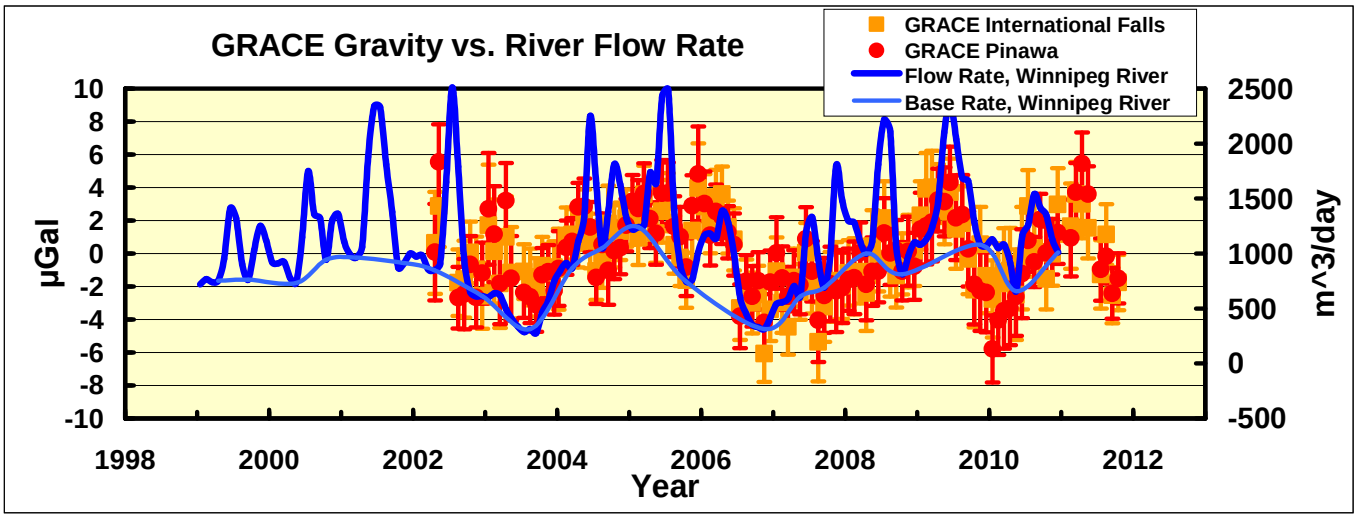

Figure 17b. GRACE monthly gravity values at International Falls, Minnesota and Pinawa, Manitoba compared to flow rates at Pine Falls on the Winnipeg River.

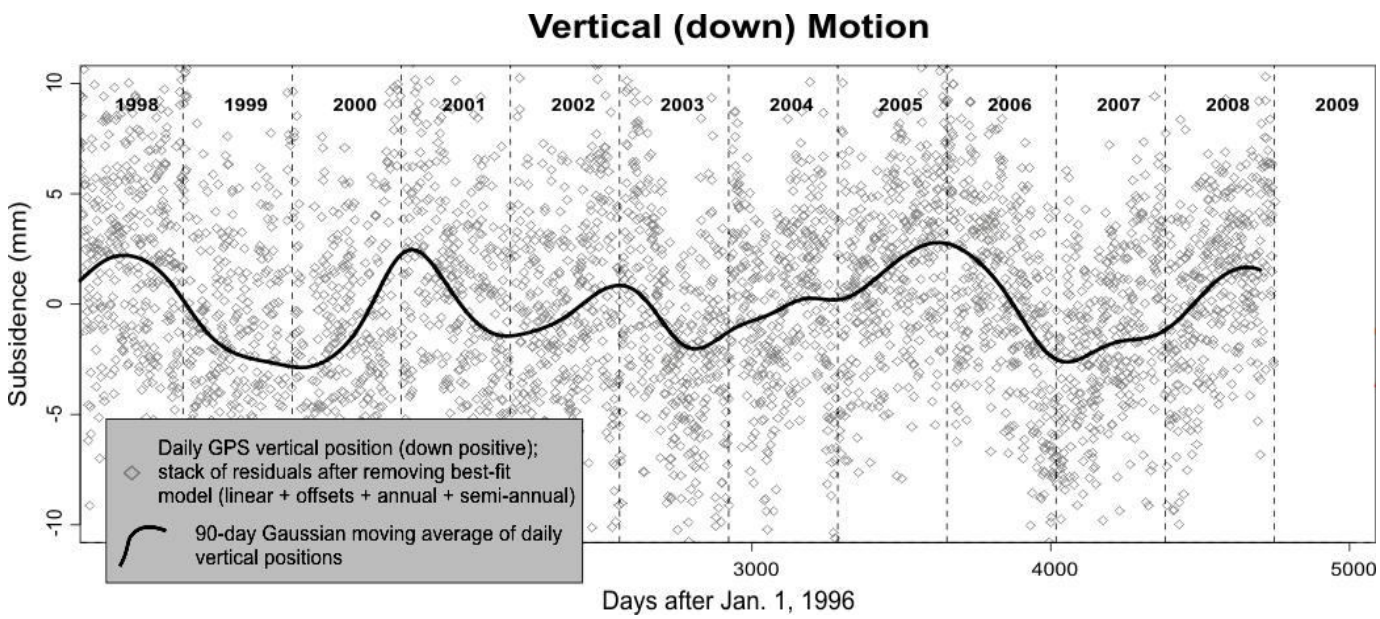

Figure 18. An average of GPS vertical observations at four sites surrounding the Winnipeg River basin.

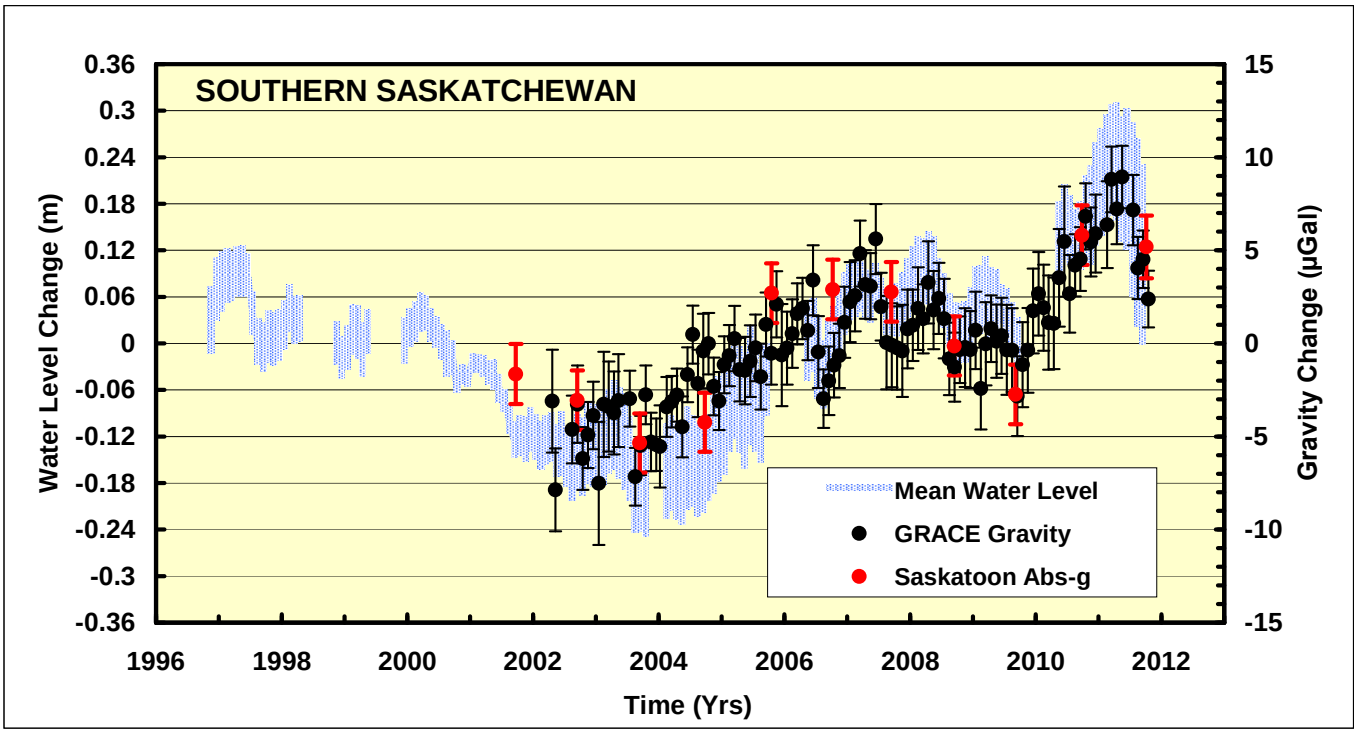

Figure 19. **S**urface absolute gravity observations at Saskatoon corrected for the long-term trend in GPS height compared with the average water-level ± its standard error from four geological weighing lysimeters north, west and south of Saskatoon and with GRACE observations centred at the centroid of the lysimeter array. The left and right vertical scales are chosen according to the theoretical attraction of an infinite layer of water (1 cm H_2O = 0.419 µGal).

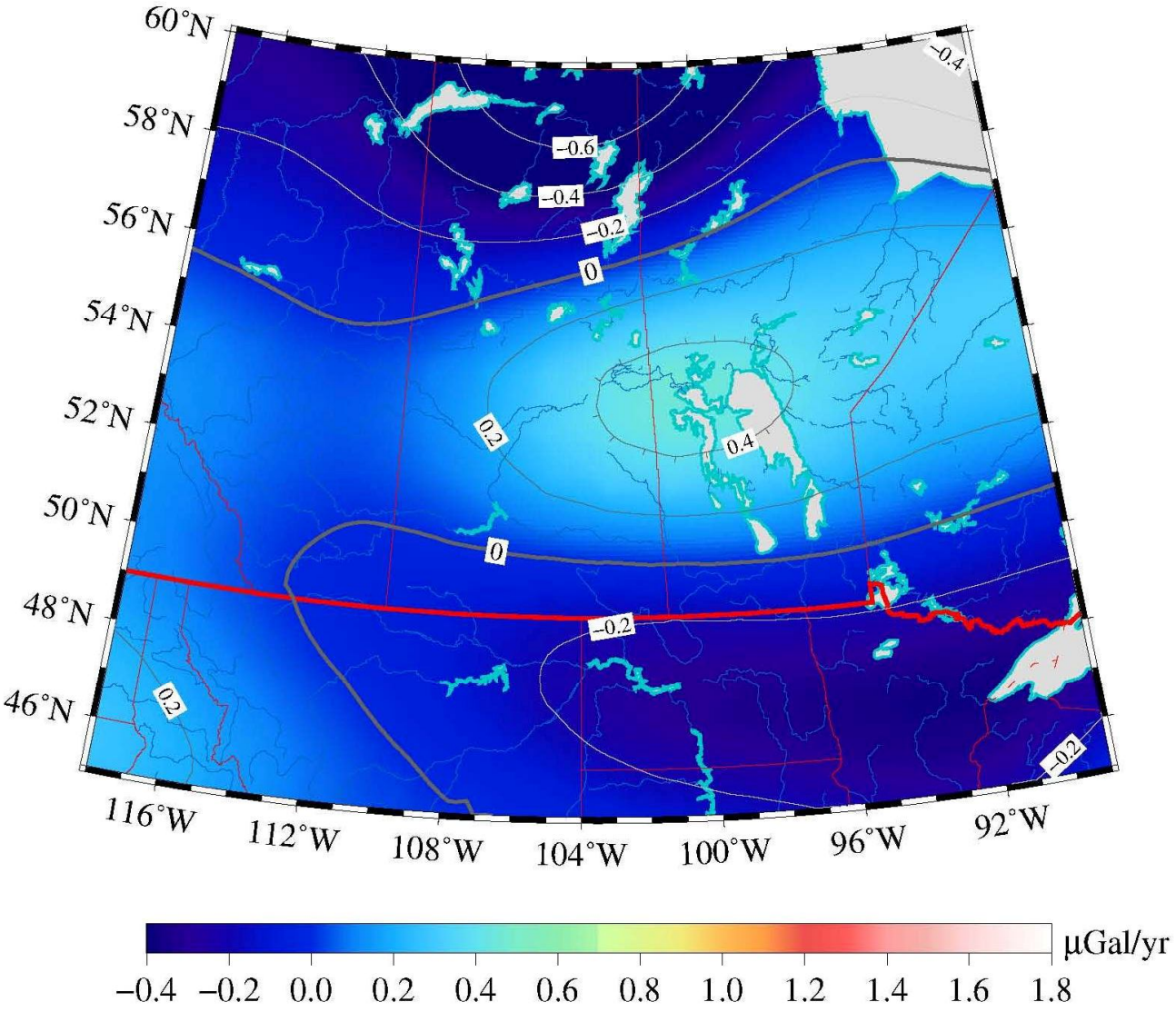

Figure 20. Equivalent gravity change estimated from the GLDAS NOAH025 soil moisture and snow model.

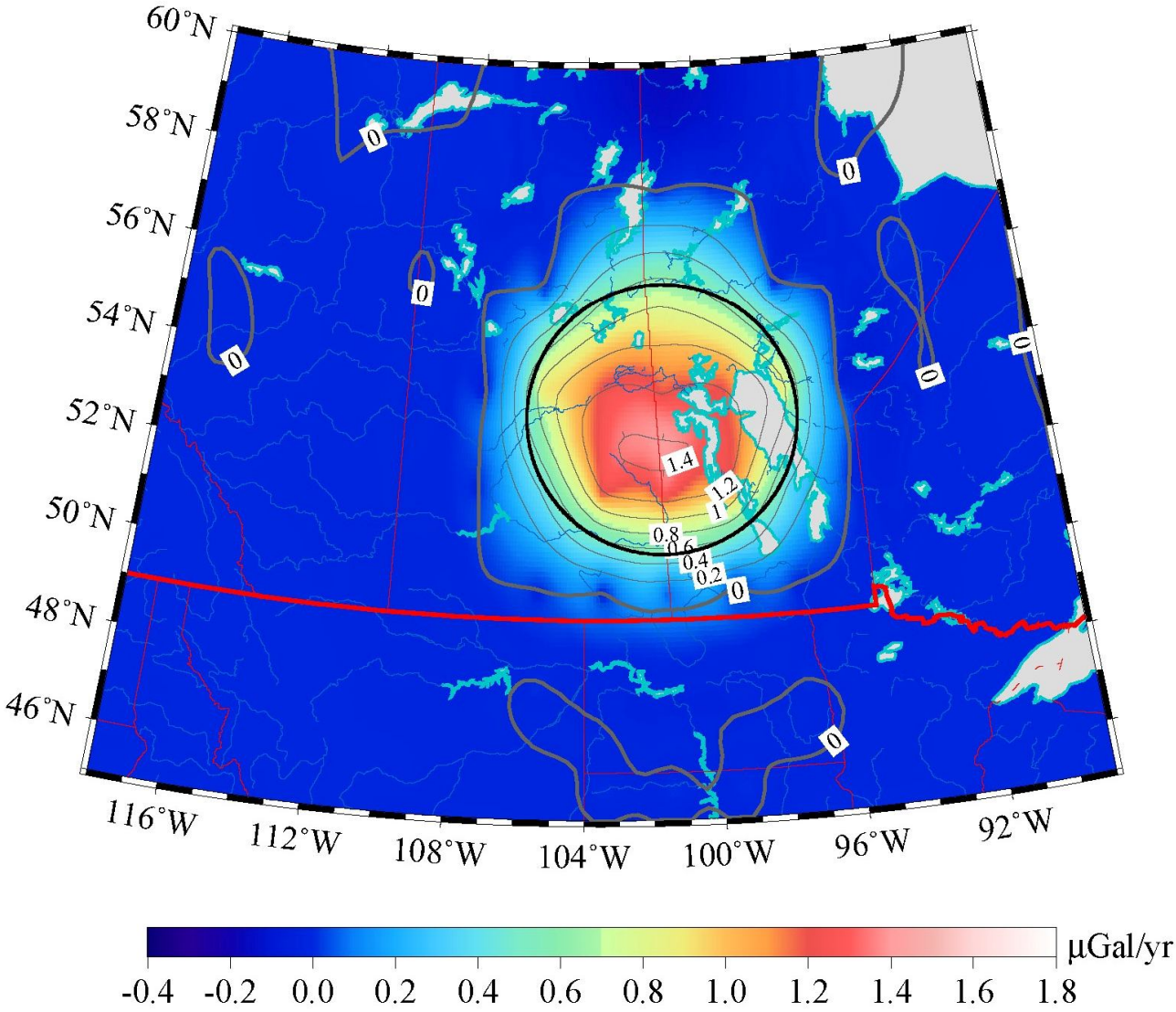

Figure A1. Gravity anomaly generated by a hypothetical spherical cap water load 300 km in radius and 3 cm thick (black circle) expressed in spherical harmonics of degree and order 2 to 256.

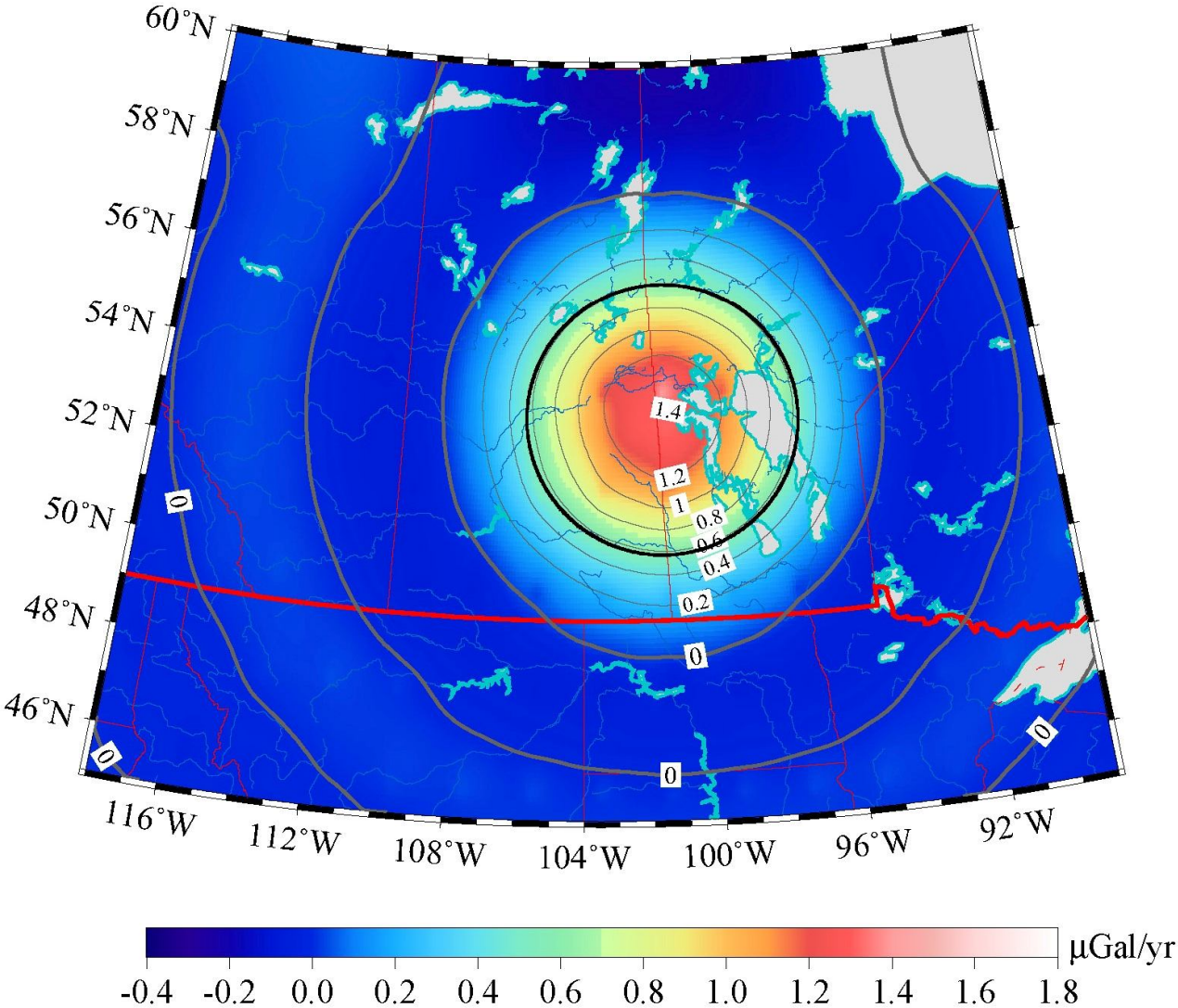

Figure A2. Gravity anomaly generated by a hypothetical spherical cap water load 300 km in radius and 3 cm thick (black circle) expressed in spherical harmonics of degree and order 2 to 60.

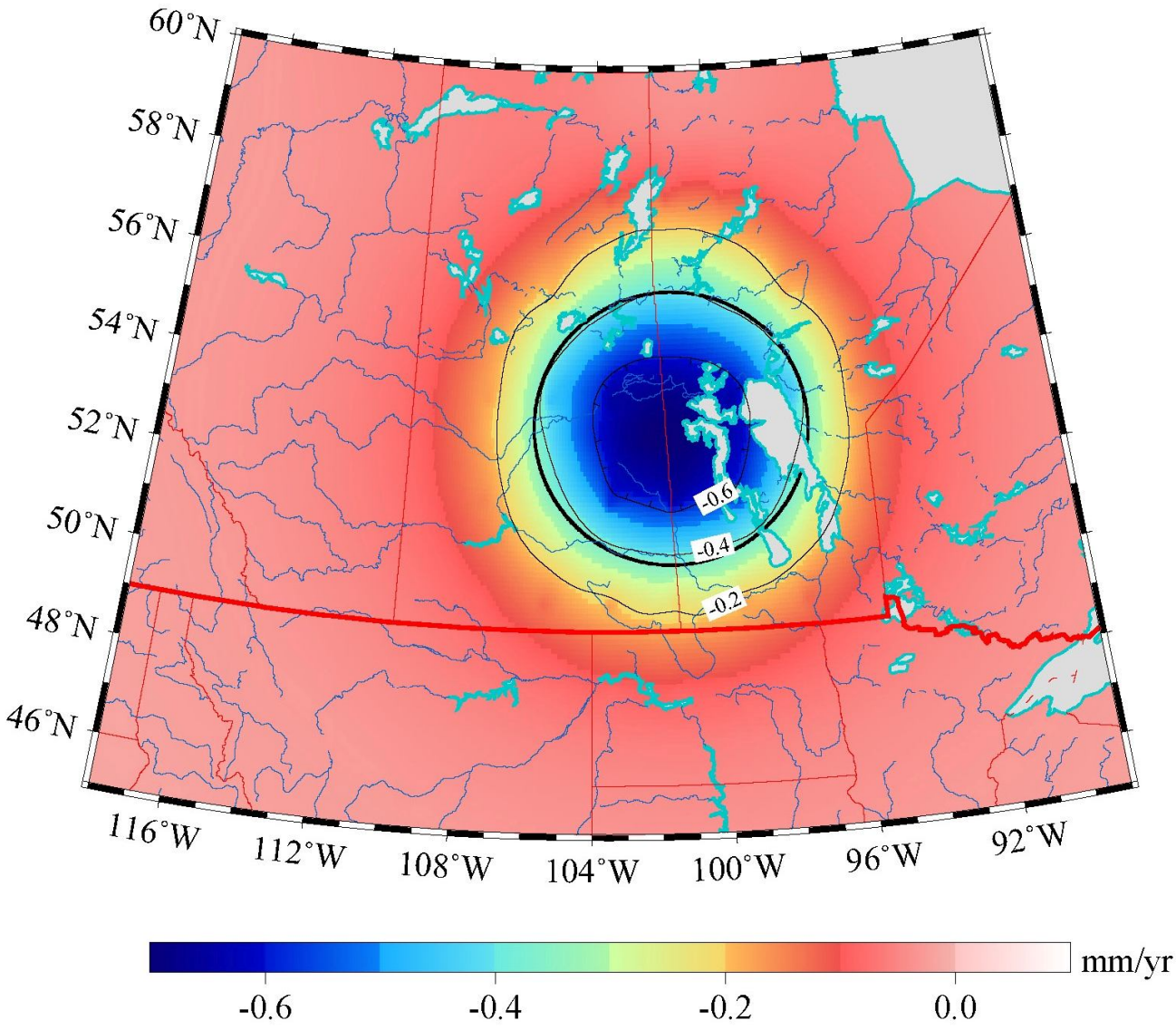

Figure B1. Vertical elastic displacement velocity (mm/yr) expected from a spherical cap water load 300 km in radius, increasing at a rate of 3 cm/yr, expressed in spherical harmonics of degree and order 2 to 256.

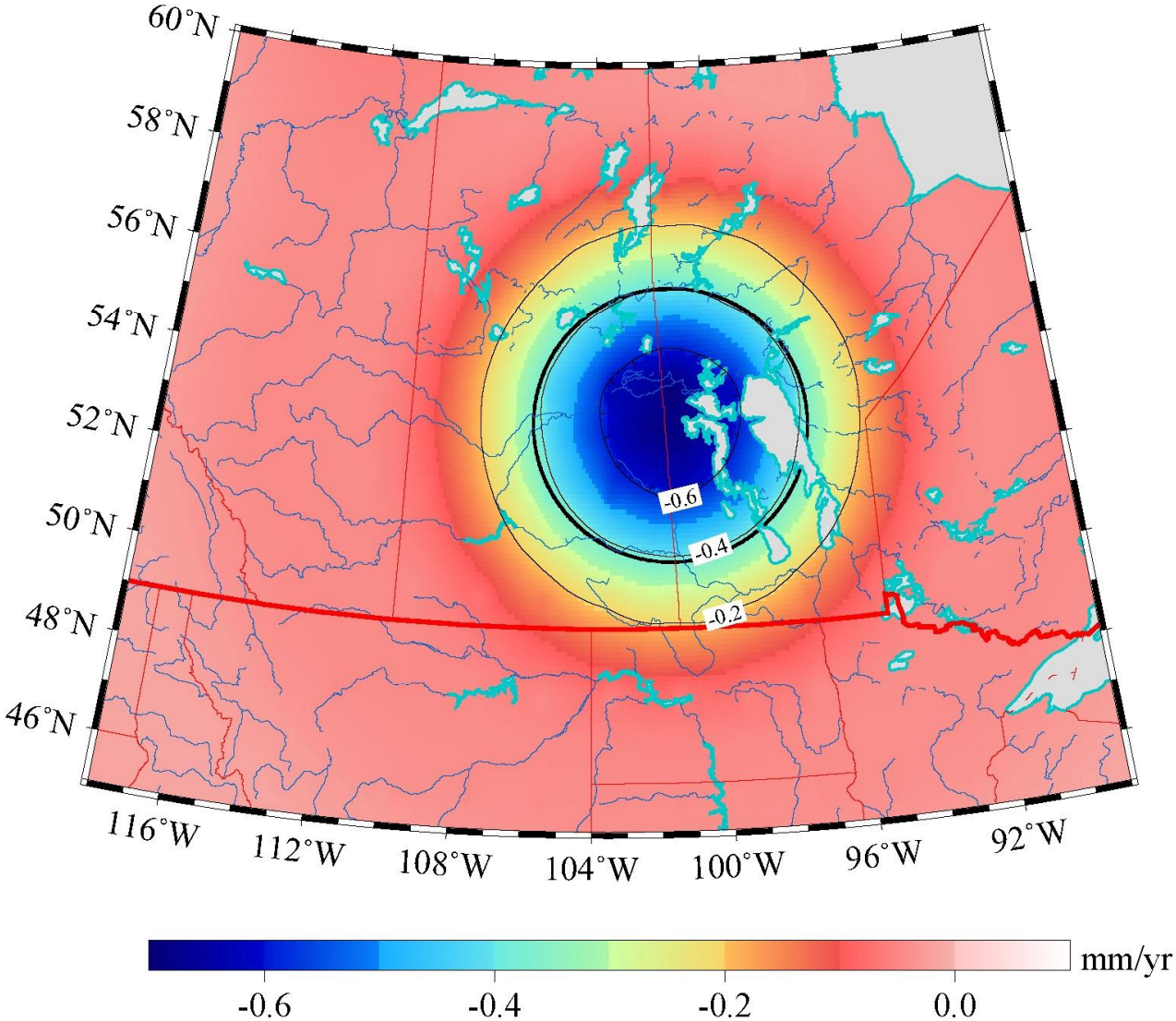

Figure B2. Vertical elastic displacement velocity (mm/yr) expected from a spherical cap water load 300 km in radius, increasing at a rate of 3 cm/yr, expressed in spherical harmonics of degree and order 2 to 60.

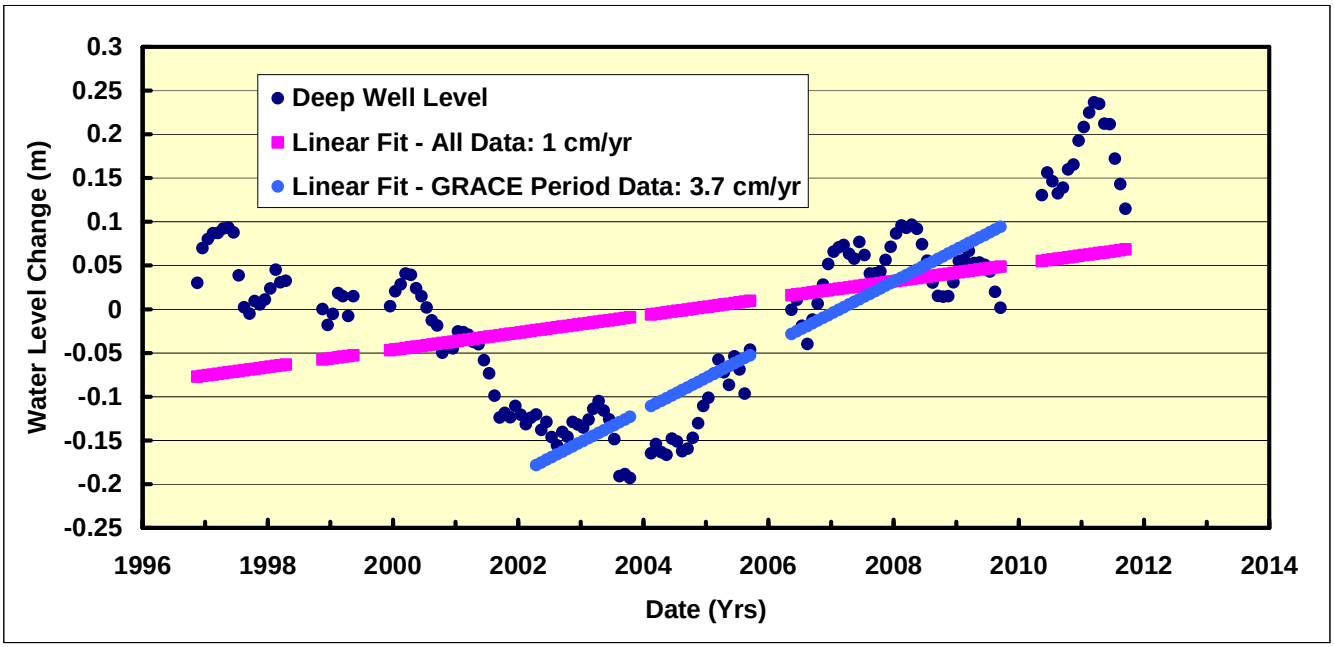

Figure B3. Comparison of mean rates of water accumulation in Saskatchewan over two different time periods: the period of GPS data input to the vertical velocity map (pink) and the period of analyzed GRACE data (blue).